Ahmad *et al. Soft Sci* 2022;2:11
DOI: 10.20517/ss.2022.08

Soft Science

Review Article

Open Access

Check for updates

A systematic review of fused deposition modeling process parameters

NurFarrahain Nadia Ahmad[1,2], Yew Hoong Wong[1,*], Nik Nazri Nik Ghazali[1]

[1]Department of Mechanical Engineering, Faculty of Engineering, Universiti Malaya, Kuala Lumpur 50603, Malaysia.
[2]School of Mechanical Engineering, Faculty of Engineering, Universiti Teknologi Malaysia, Johor Bahru, Johor 81310, Malaysia.

[*]**Correspondence to:** Prof. Yew Hoong Wong, Department of Mechanical Engineering, Faculty of Engineering, Universiti Malaya, Wilayah Persekutuan Kuala Lumpur, Kuala Lumpur 50603, Malaysia. E-mail: yhwong@um.edu.my

How to cite this article: Ahmad NN, Wong YH, Ghazali NNN. A systematic review of fused deposition modeling process parameters. *Soft Sci* 2022;2:11. https://dx.doi.org/10.20517/ss.2022.08

Received: 25 Apr 2022 **First Decision:** 23 May 2022 **Revised:** 8 Jun 2022 **Accepted:** 13 Jun 2022 **Published:** 13 Jul 2022

Academic Editors: Zhifeng Ren, Cunjiang Yu **Copy Editor:** Fangling Lan **Production Editor:** Fangling Lan

Abstract

Fused deposition modeling (FDM) is an additive manufacturing technique with significant advantages, including cost effectiveness, applicability for a wide range of materials, user-friendliness and small equipment features. However, its poor resolution represents a hindrance for functional parts for commercial production. In this review, the key process parameters are presented with their factors and effects on the characteristics of FDM-printed polymeric products. Hence, better insights into the relationship between key parameters and three main printing characteristics, namely, surface roughness, mechanical strength and dimensional accuracy, in existing FDM research are provided. A conclusion that addresses the challenges and future research directions in this area is also presented.

Keywords: Additive manufacturing, fused deposition modeling, process parameters, polymers, characteristics

INTRODUCTION

Industry 4.0 has encouraged the development of advanced additive manufacturing technologies[1,2] with the ability to simplify a whole fabrication process into one step, produce complex designs, reduce the production cycle time and cost[3] and increase the reproducibility. This development has therefore enabled their wide application in the pharmaceutical, biomedical, soft robotics, flexible electronics, aerospace, automotive and architectural industries. Fused deposition modeling (FDM) has gained significant

popularity as it has important advantages, such as being cost-effective in terms of the printer and material used, a wide range of applicable thermoplastic materials and user-friendly and small equipment features[4]. However, its applications, especially regarding functional parts, are limited because of its poor resolution[5] that effects the surface quality and poor mechanical strength and dimensional accuracy. These limitations represent strong hindrances to commercial production, which requires adequate high-precision and stable qualities to meet product requirements.

Numerous researchers have carried out studies to analyze the key parameter effects to achieve desirable properties for FDM-printed products[6-9], with many of them using various statistical tools. A large number of conflicting FDM parameters that influence the characteristics of the printed product are impediments in determining the optimal parameters to use[10,11]. Although the effect of FDM process parameters has been extensively covered in recent studies[2,6-8], none of them have visualized the factors of parameter selection, direct-indirect effects and their relationship in a systematic manner for better understanding.

In this systematic review, the research related to FDM process parameters from 2013 to 2021 is used as a reference. In Section 2, a brief explanation of the definition, factor and effect of key parameters is presented, before further focusing on their relationships toward the characteristics for fabrication. To demonstrate a better understanding of the influence of key process parameters on multiple part characteristics, an overlap mind map and graphic illustration are provided. In Section 3, three main effects on characteristics, namely, surface roughness, mechanical strength and dimensional accuracy, are discussed in detail. In Section 4, the remaining significant challenges, which contribute to the part characteristics, are discussed. In section 5, the current progress is addressed and the overall findings are concluded.

Overview of FDM process

FDM is a technique that utilizes a heating element to heat up a continuous filament made of a thermoplastic polymer from a solid to a molten state, which enables layer-by-layer material deposition via a moving nozzle head and solidifies after cooling to room temperature to build the part. The filament material should be sufficiently stiff and rigid during the extrusion process to prevent buckling owing to the pressure generated during the feeding process. The thermoplastic filament extruded through the printing nozzle displays viscosity levels that are sufficiently low to assure the flowability of the melt. When semi-liquid thermoplastic filament materials are extruded from a nozzle on the printing platform, they do not immediately solidify. Instead, these semi-liquid thermoplastics, for a specific layer under construction, fuse together before curing/solidifying into a layer-wise stacked part at ambient temperature. In the post-deposition stage, one layer remains molten, lying at the interface between adjacent deposited layers must able to interdiffuse across the interface, to ensure a good level of interlayer adhesion due to the molecular interactions. Figure 1 illustrates FDM and the main features required for proper material extrusion[12].

The FDM process commences with a relevant slicer software. Firstly, a three-dimensional (3D) digital model is created with any design software, such as Solidworks, Catia, Rhino or Inventor, and the design is finalized with optimization using computer-aided design (CAD) and analysis software according to the printer specification. The 3D digital model is then converted to a printer recognized format file (e.g., a stereolithography file or OBJ). The file is imported into the printer software and the model to be printed is configured. Slicing software is utilized with all the printing requirements are included. This configuration contains the material selection and the nozzle size of the printer. The software also separates the model into layers and the printing quality and movement commands can be configured. The specific procedure for fabrication is carried out according to its working principle and layer-by-layer printing is developed until the complete fabrication of the 3D printed model.

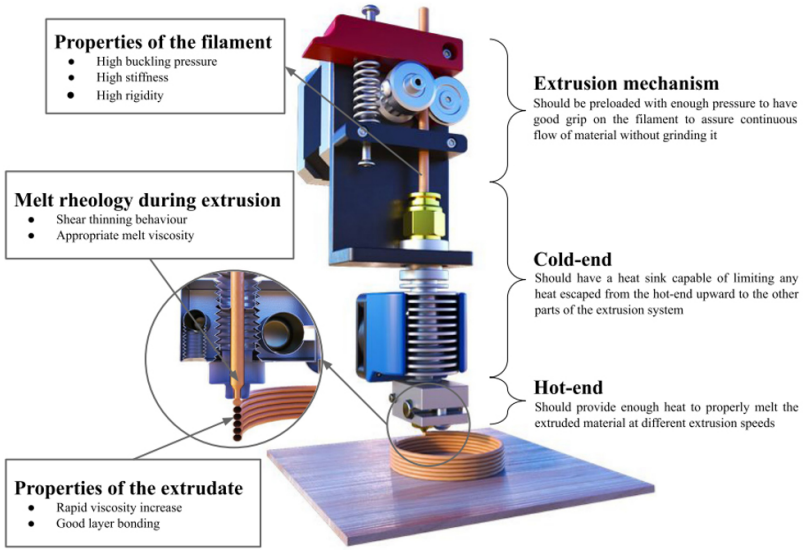

Figure 1. Fused deposition modeling diagram, reproduced with permission[12], Copyright 2021 Springer.

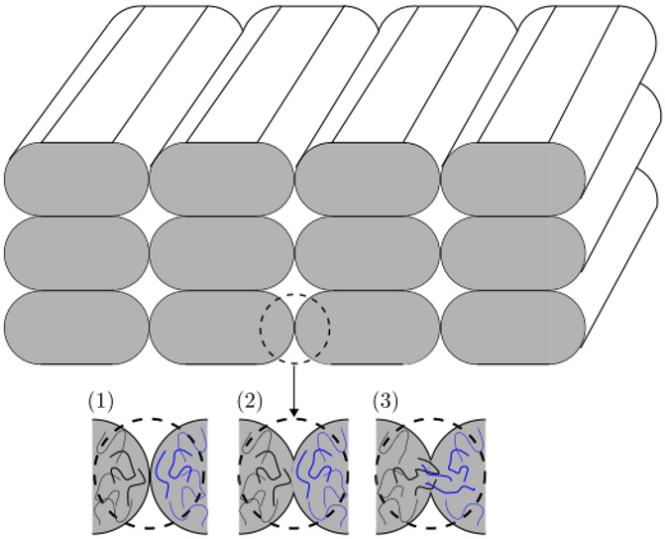

Figure 2. Bond formation process through sintering: (1) surface contact; (2) neck growth; (3) neck growth and molecular diffusion at the interface, reproduced with permission[15], Copyright 2020, Elsevier.

Bond formation mechanism

The thermal energy of the semi-molten material drives the development of bonding in the FDM process. The degree of interlayer and intralayer bonding is critical in determining the characteristics of the product[13]. In the solidification process, the cross sections of the beads are originally idealized as circles. Their molecules generate interfacial molecular contact through wetting [Figure 2(1)] and then move toward preferred configurations to achieve adsorptive equilibrium. Molecules diffuse across the contact, generating an interfacial zone and/or reacting to form primary chemical bonds across the interface[14]. A neck growth is formed [Figure 2(2)], which is a kind of bridging formed by viscous sintering between two adjacent beads. The magnitude of neck growth and molecular diffusion reflect the quality of the bond formation [Figure 2(3)][15]. The intra- and interlayer bonds and neck size all influence the part strength. The sintering is the phenomenon involving coalescence of the particles and is mainly driven by two temperature-

dependent properties which is surface tension and viscosity.

Application of FDM products

This manufacturing technology offers a broad range of part production options due to its ability to create complicated parts and their flexibility. FDM may be used to produce a variety of applications that require rapid and affordable parts or rough and stiff products for end customers. The following examples illustrate some of the available parts with their applications that were fabricated by FDM:

In the aerospace industry, including aircraft, drone parts and rockets, FDM manufactured parts are used to replace traditional metal components that can reduce their weight whilst maintaining appropriate robustness and reducing the turnaround time for part repair. Stratasys adopted FDM for rapid prototyping, manufacturing tooling and part production in collaboration with various aerospace companies, such as Piper Aircraft, Bell Helicopter and NASA. For example, NASA printed 70 components of the Mars rover using Stratasys FDM technologies to obtain a lightweight and strong structure. Bell Helicopter manufactured polycarbonate wiring conduits for their V-22 Osprey using FDM whilst reducing the manufacturing time to 2.5 days (from 6 weeks)[16]. Stratasys and Aurora Flight Sciences utilized ULTEM 9085 resin and FDM technology, where a honeycomb internal structure was used inside the internal wing design. Boeing uses FDM parts for its 777-300 ER door handles and camera cases.

In architecture, the first 3D printed residential construction, known as the 3D Print Canal House, was built in Amsterdam in 2014 by Dus Achitects using the FDM process. The house was printed using a thermoplastic material (a biodegradable plastic in this case). The project managed to demonstrate the mobility of the printer, how 3D printing could revolutionize construction by increasing the efficiency and the rapid building of low-cost housing whilst reducing pollution and waste[17].

FDM has also been used to assist with personalized medicine and customizable implants for various medical applications. Customized tracheal stents fabricated by FDM are less expensive and have better surface quality[18]. An anatomically shaped lumbar cage for an intervertebral disc fabricated by FDM was physically characterized to ensure its compatibility for load bearing applications as a spinal implant[19]. In addition, FDM has been extensively used for scaffoldings and tissue engineering. In the pharmaceutical industry, FDM, in combination with hot-melt extrusion (HME) and optimized formulation compositions, has recently proven to be a viable solution for the production of pharmaceutical tablets and implants with variable drug release patterns. We refer the reader to the latest reviews from Caileaux *et al.* and Chen *et al.* for further details on these applications[20,21].

PROCESS PARAMETERS IN FUSED DEPOSITION MODELING

The main process parameters are described below and depicted in Figure 3[22,23].

Nozzle diameter

The nozzle diameter is the diameter of the extruder tip and depends on the type of nozzle used[24]. The extruder nozzle diameter has an impact on the extruded melt flow behavior. Basically, the filament encounters a high shear rate at the nozzle and a low shear rate when deposited on the bed during the FDM process. The pressure drop can increase due to flow instabilities caused by variations in shear rate throughout the nozzle diameter[25]. The selection of an optimal nozzle diameter is critical for maintaining a proper and consistent flow of the extruding material. As the outlet nozzle diameter becomes narrower, the pressure drop increases[26]. Compared to a narrow diameter, the pressure drop caused by larger nozzle diameters provides consistency of the applied raster width and thus affects the accuracy of the finished

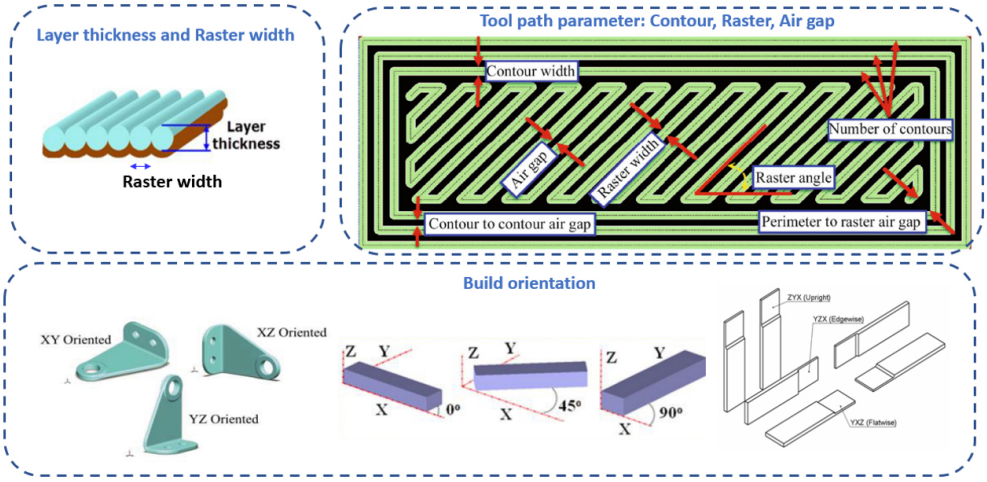

Figure 3. Illustrations of process parameters, including layer thickness and Raster width, build orientation and FDM tool path parameters. Layer thickness and Raster width, reproduced with permission[22], Copyright 2022, Springer. Build orientation, reproduced with permission[23], Copyright 2017, Springer. FDM tool path parameters, reproduced with permission[11], Copyright 2015, Springer.

printed parts. The decrease in the nozzle diameter contributes to better resolutions with low layer thickness, which in turn provides a good surface quality. The recommended guideline for the maximum layer height is not more than 80% of the nozzle diameter. This is because the extruded materials need to be pressed in order to fuse them. The larger the nozzle diameter, the shorter the time it takes to complete the item.

Although there was no linear correlation, a larger nozzle hole diameter was found to increase the density and tensile strength of the products[27]. By increasing the nozzle diameter, more molten material may be deposited to fill the volume, causing the product to become solid with a narrow distance between infills. The small nozzle diameter demonstrates that the distance between infills has a wide gap, resulting in many voids between layers. The tensile strength of the printed product increases as the interlayer cohesion is increased when using a low layer thickness via a smaller nozzle diameter.

Extrusion and bed temperature

The extrusion temperature is the temperature used to convert the solid filament into a molten state before the extrusion process and depends on the material type and printing speed. It should be set based on the melting point of the filament material[28]. The bed temperature is the temperature of the heating element that places the printed product model[29]. During the extrusion process, the thermoplastic materials are in a viscoelastic state and the high temperature enables the stretching and alignment of polymer chains in the direction of the material flow through the extrusion nozzle. The material begins to cool and solidify as soon as it exits the extrusion nozzle. The hot material from the extruder nozzle is deposited onto the previously extruded layer, which, in the process of cooling, causes the latter to reheat. Rapid heating and cooling can cause non-uniform thermal gradients and increase the internal stress, which will pull the underlying layer upward and cause it to distort.

The extrusion and bed temperatures are related to the dynamic cooling of viscous polymer melts. Thus, the final properties of the printed parts are dependent on the stress relaxation and polymer chain diffusion in this cooling process, which can have a positive influence on the part quality and its strength. The temperature increases around the crystallization temperature at the interface of the adjacent bead, allowing appropriate bonding to form. The previously deposited layer should be sufficiently heated around the crystallization temperature to allow for molecular chain rearrangement during deposition of the melting

filament. The higher temperature of the previously deposited filament could cause the molten material to rapidly flow and the deformation of subsequent deposited layers to occur. At lower temperatures, the molecular chain of the deposited material does not have sufficient time to be rearranged and undergo stress relaxation, thereby causing lower bonding of the two adjacent beads.

Heated beds help to prevent rapid residual stress relaxation during the printing process due to a change in the ambient temperature. This leads to different thermal effects on the quality of the build parts. The quality of the printed parts is also dependent on the diffusion at the joints among the beads, which is dependent upon the shape of the beads and might be caused by the direction of the heat transfer. Basically, the heat transfer occurs from the higher temperature region to a lower temperature region. Smaller differences in the bed and ambient temperatures can reduce the thermal gradients, resulting in shape errors caused by the decreased heat shrinkage of the printed product. It is noteworthy that the bed temperature should be as close to the material softening temperature as possible in order to minimize warpage or shrinkage due to thermal stress reduction. The printing bed should be heated to a certain temperature range to improve adhesion and prevent deformation caused by shrinkage during the solidification process.

Print speed

The print speed is the distance travelled by the nozzle tip per unit time (mm/s) during the printing process. The optimum printing speed in FDM is determined by the material, extrusion temperature and resolution used.

Higher printing speeds result in smaller heat transfer windows, which might lead to the extrusion of a partially melted extrudate. This has a significant impact on the dynamic cooling and melting rates of a material, resulting in poor layer bonding. Setting a high printing speed might lead to poor layer bonding and, as a result, a reduction in the mechanical strength of the product. Faster printing speed results in larger voids and worsened interlayer bonding. Lowering the printing speed means sacrificing the build time and printing efficiency.

To minimize melting instabilities, the nozzle temperature and printing speed should be compatible, i.e., if the extrusion temperature is too high at a slow printing speed, the melt becomes less viscous, reducing the dimensional stability and increasing the cooling time. Similarly, if the set temperature is too low at high speeds, the filament may not melt as quickly as it should (due to materials becoming stuck inside the nozzle), resulting in a melt that is much more viscous than it should be. The shrinkage issue can be reduced by using appropriate combinations of nozzle temperature and printing speed.

Build orientation

The build orientation is defined as the mode position part that is placed on the platform in respect of the X, Y and Z axes and can be presented as a quantitative parameter (angle of axis) or a categorical parameter (ZX-upright, XZ-edgewise and XY-flatwise). The selection of the optimum building orientation is determined based on the user's selections of primary criteria and takes geometrical factors into account: minimizes the support structure volume and contact area. For different build orientations, the build time and number of layers required are determined. The build time increases when the build orientation changes from flat to upright. This is because the number of layers for this build orientation is significantly greater and the required build time and material used for the upright build orientation increase. This leads to an energy usage increase and higher energy costs. The part build orientation is the most important process parameter, which has a significant impact on the surface finish, dimensional accuracy, mechanical strength and post-processing requirements.

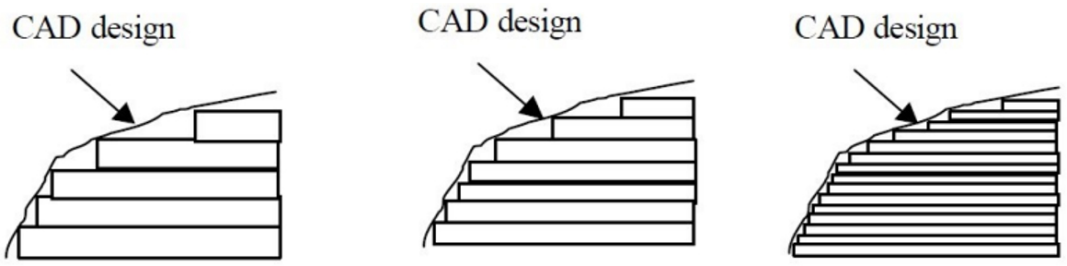

Figure 4. Comparison of staircase effect for various layer thicknesses, reproduced with permission[30], Copyright 2000 Researchgate.

The staircase effect is minimized if the build orientation is parallel or vertical to the surface facet of the printed model. If the angle between the surface normal and the build orientation (range of 0°-90°) increases, the staircase effect is noticeable and the surface quality decreases. The areas of the part that are frequently smoothed by the extrusion nozzle but are not directly in contact with the support material and build platform achieve a fine surface finish. As a result, a 3D printed part is actually a top-facing surface and will always have a low surface roughness. As the build orientation can vary the number of layers, edge errors and layer swelling, which have an impact on the dimensional accuracy, can be avoided by properly placing the component. The build orientation affects the layer-by-layer bonding inside the printed product and can resist the load when oriented in the load direction. If the load is applied horizontally in the 0° orientation printed part or applied vertically 90° orientation printed part, the weaker bonding leads to strength failure. In addition, post-processing is required to minimize aesthetic defects due to adhesion forces that are related to the heated bead.

Layer thickness

The layer thickness is defined as the vertical resolution and depends on the material, nozzle diameter and type of nozzle and can influence the surface quality, dimensional accuracy, mechanical strength and build time.

While a low layer thickness will result in a good surface finish, a high layer thickness will result in a poor surface finish. This is because when the layer thickness increases, the number of layers will decrease, making the staircase effect more obvious [Figure 4][30]. It is difficult to preserve the geometry inaccuracy between the printed product and the original CAD dimensions due to the staircase effect. A low layer thickness is preferable for improving the dimensional accuracy. The effect of layer adhesion on the strength of a printed object is determined by how well the individual layers of the material stick together. Thinner layers may be stronger because a shorter distance between the nozzle and the preceding layer may heat the material and a smaller amount of material aids the homogeneous heat distribution, leading to effective bonding formation. Furthermore, since the gaps between the lines of an already printed material are smaller, the density of the parts with thinner layers may be larger, leading to a stronger structure. The stiffness and strength of an FDM-printed part are not only a function of the void density but also of the number of layers[31]. The build time is inversely proportional to the layer thickness. More build time is required for a low layer thickness.

Raster width and angle

The raster width is defined as the road width and depends on the nozzle diameter. A smaller raster width requires more production time and less material consumption. Larger raster widths give greater bonding area, which may increase the diffusion and result in stronger bonds[32]. However, a larger raster can also result in stress accumulation along the width of the part and a deterioration in the thermal distribution[33]. The thermal mass of a larger raster may be attained, allowing it to cool more slowly, which increases the

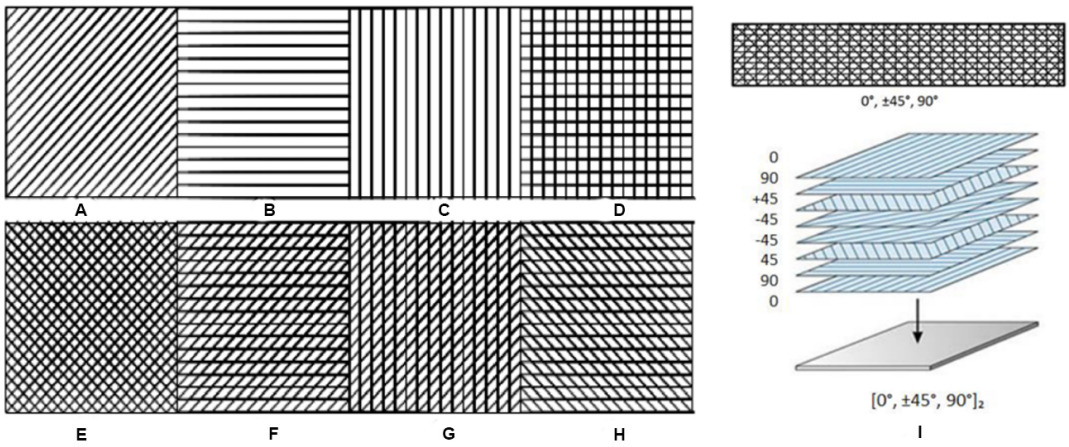

Figure 5. Representative examples of raster angles/orientations: (A) +45°; (B) 0°; (C) 90°; (D) 0°/90°; (E) +45°/-45°; (F) 0°/+45°; (G) 90°/+45°; (H) 0°/-45°. (I) Combination of 0°/+90°/+45°/-45°/-90°/0° Reproduced with permission[2,36], Copyright 2020, Elsevier and Copyright 2013, Thesis from Worcester Polytechnic Institute.

bonding between the beads and therefore enhances their strength[34].

The raster angle is defined as the viewpoint of the raster path with respect to the X axis in the printing platform that is attributed to the internal structure of the final printed product. The raster angle has an influence on the surface roughness and mechanical strength. The surface roughness is measured in the parallel and perpendicular directions to the tensile loading. Surface roughness values are lower when the measuring direction is parallel to the raster angle of 0° and the tensile loading. When measuring the tensile strength perpendicular to the tensile loading and parallel to a raster angle of 90°, the lowest surface roughness is obtained. From a mechanical strength point perspective, the fracture initiated from the edge and propagated until a complete fracture occurred. The crack propagates in the transverse direction to the applied force at a 0° raster angle and fracture occurs owing to the raster failure. The fracture path is also transverse to the applied force at the raster angle of 90°; however, the fracture occurs between the interlayer bonds. The interlayer bonding strength is significantly lower than the strength of the raster, which explains the higher tensile strengths obtained for the 0° raster angle[35]. The impact of the raster angle on the build time is still unknown.

Figure 5 illustrates representative examples of the different raster angles[36].

Air gap

An air gap is defined as the spacing between two adjacent deposited beads in the same layer and can be categorized into three types of gaps, namely, positive, negative (overlap between two adjacent layers) and zero gaps. Positive air gaps allow for spacing between two adjacent layers, resulting in a loose interconnection structure with weak bonding between adjacent filaments, leading to lower strength. A negative air gap refers to the overlap position of two beads with strong interfacial bonding, significantly improving the strength. A zero gap means that the beads are touching each other and this type of printing is highly recommended. The roughness value improves with the reduction of the air gap[37]. There is a space between the adjacently laid roads when there is a positive air gap. When a semi-liquid material is extruded, it might flow in an unexpected manner through the gap, causing surface variance. In a negative air gap, bump formation occurs, resulting in an uneven surface. In a zero-air gap condition, the beads are close to each other, which restricts the flow and fusion in the predicted manner.

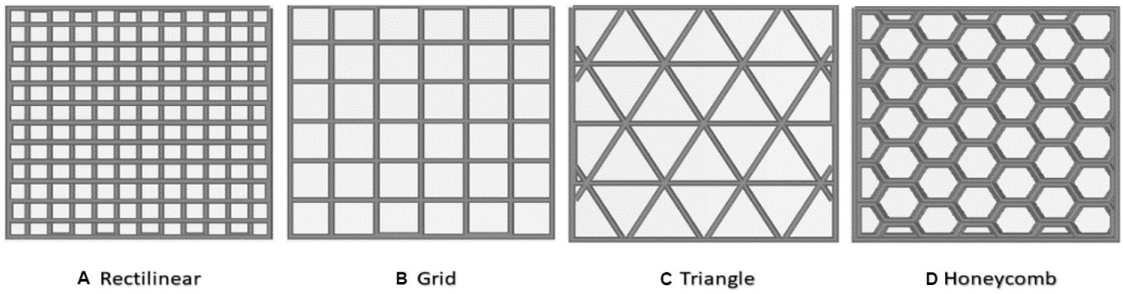

Figure 6. Representative infill patterns: (A) rectilinear; (B) grid; (C) triangle; (D) honeycomb, reproduced with permission[38], Copyright 2020 Elsevier.

Infill density and pattern

The infill density is defined as the percentage of material consumption used to build the internal structure of a printed product. The air gap and raster width parameters allow users to control the infill density. The density of the infill influences the mass and strength of an FDM-printed part. Lower densities require less print time and material, resulting in cost savings and weight reduction. However, when more voids are formed within the structure simultaneously, the porosity increases. Thus, the bonded area decreases as a result, resulting in poor mechanical characteristics. In contrast, the denser component has higher mechanical qualities but takes significantly longer to complete.

The infill pattern illustrates the internal geometrical layout of the printed part [Figure 6][38]. The complexity of the infill pattern affects the print time, material consumption and mechanical characteristics. For example, in the hexagonal design, each layer is laid down similarly on top of a previous layer, just like the bonding zone. In contrast, in the rectilinear pattern, the new layer crosses the previous layer at places that correspond to the bonding zone between each layer. Therefore, the design of the cross in rectilinear has higher tensile strength compared to the honeycomb pattern.

Based on a literature review, Figure 7 demonstrates a simple mind map of key parameters for better understanding.

PREVIOUS RESEARCH OF PROCESS PARAMETER OPTIMIZATION AND ANALYSIS

The process conditions must be established for each application in order to fulfill the customer needs and satisfaction. FDM has a large number of conflicting parameters that influence the part characteristics individually or in combination. Determining the optimal conditions of process parameters is critical for a significant impact on production efficiency and part characteristics. There have been tremendous research efforts to identify the influence of FDM process parameters on surface quality, mechanical strength and dimensional accuracy.

Surface roughness

Surface roughness is extensively used as an index of product quality. The staircase effect is one of the main problems in additive manufacturing to achieve good surface quality. The layer-by-layer appearance not only effects the aesthetic view but its surface characteristics are also important to ensure proper function in terms of dimensional precision and stress concentrations that can cause early failure under fatigue loading. Surface defects that may exist in FDM include the chordal effect, the residue of access material that appears between lines[39], support structure burrs and errors due to the starting and ending of deposition, leading to a poor surface finish. ASTM B46.1 is a common test to measure surface roughness and average of the absolute value of profile heights over a given length (area) are calculated. Setting optimal process

Figure 7. Mind map of factors and direct/indirect effects of process parameters. (A) Nozzle diameter; (B) extrusion temperature; (C) bed temperature; (D) print speed; (E) build orientation; (F) layer thickness; (G) raster angle; (H) raster width; (I) air gap; (J) infill density; (K) infill pattern.

parameters, either individually or in combination, can improve the surface quality of the printed part. Table 1 shows the research studies that investigated the influence of key parameters on the surface roughness in FDM printing. A detailed explanation for each important parameter is presented as follows:

a. Effect of layer thickness on surface roughness: The surface finish of an FDM-printed product is improved by decreasing the layer thickness. The findings of Ayrilmis *et al.* regarding the layer thickness relationship with surface roughness contradict the findings of Reddy *et al.* who found that a high layer thickness leads to a better surface finish[40,41]. As layer thickness increases, amplitude and spacing of the surface profiles increases and the stair-stepping effect decreases.

b. Effect of build orientation on surface roughness: The surface roughness increases as the build orientation angle increases[42,43]. The selection of build orientation depends on the complexity of the design that might require a supporting material for printing. A preferable build orientation is to be printed in the smallest dimension or shortest side of the target model with respect to the Z direction of the build platform, as the top surface that is extruded by the nozzle is smooth compared to the region that is in contact with the print bed, which normally has a support mark.

c. Effect of print speed on surface roughness: The surface quality in both the horizontal and vertical directions is reduced when the printing speed increases. Slow printing speeds lead to better surface quality because they can provide more time for material deposition and fusion processes. At higher speeds, there is potential for the material not to deposit effectively and the time taken for the thermoplastic chains to diffuse and crystallize is reduced, leading to a rough quality surface. There is also a risk of deposited bead stacking up at high print speeds. The extrusion of a material is inhomogeneous and insufficient at high print speeds. The amount of material deposition significantly influences the surface topography using a layer thickness of 0.2 mm, as shown in Figure 8[44].

d. Effect of extrusion temperature on surface roughness: An increment in the extrusion temperature decreases the surface roughness, which is due to a reduction in viscosity. The low viscosity leads the extruded bead to lose shaping control (the desired shape is a sectional circular shape) and form an oval shape. The oval shape generates a wider contact area between layers, resulting in low surface roughness. The higher temperature produces more bulging as more material is laid down from the nozzle and when it rounds off by the contact area between layers, better surface quality can be obtained.

e. Influence of raster-related parameters and air gap on surface roughness: The surface roughness can be reduced by increasing the raster width. For air gaps, the best condition is zero. However, in reality, even though a zero physical gap is set at the printer, it is difficult to obtain a zero physical gap. Negative air gaps (overlap condition) may reduce the surface roughness because less voids between beads result in a smoother surface construction.

f. Short discussion and summary of key parameters related to surface roughness: Layer thickness is the most favored and influential factor in FDM. According to Anitha *et al.* layer thickness has a significant impact on surface roughness, contributing 51.57%, followed by raster width (15.57%) and print speed (15.83%)[45]. Nidagundi *et al.* highlighted that layer thickness, build orientation, and fill angle contribute about 88.45%, 7.55%, and 4.09% to surface roughness, respectively[46]. The statement that layer thickness has a strong relationship with surface roughness was supported by findings from other research studies[47,48]. For both low and high layer thicknesses, there is no clear guideline for selection in achieving good surface quality. Basically, it depends on the gaps between layers being the main cause of surface roughness. The top printed

Table 1. Summary of research studies investigating the influence of key parameters on surface roughness in FDM printing

First authors	Year	Reference	Method	Mat.	Fix item	Variable item	Optimum value	Surface roughness, Ra (μm)
Ognjan Lužanin	2013	[120]	ANOVA, Half-normal plot, Residual Plots, Main Effects diagram, geometric interpretation	PLA	(1) Infill density = 15% (2) Number of contours = 2 (3) Layer thickness = 0.1 mm Print speed = 100 mm/s	(1) Extrusion temp = 225, 230, 235 °C Print speed = 40, 60, 80 mm/s	(1) Extrusion temp = 235 °C (Highest) Print speed = 40 mm/s (Lowest)	1.5511
Maruthi Prasad	2014	[121]	Full factor experiment, Box-Behnken design, ANOVA, RSM, genetic algorithm	ABS M30	(1) Air gap = 0 mm Contour width = 0.464 mm	(1) Layer thickness = 0.127, 0.178, 0.254 mm (2) Build orientation = 0, 15, 30 (3) Raster angle = 0, 30, 60 (4) Raster width = 0.4064, 0.4564, 0.5064 mm Air gap = 0, 0.004, 0.008 mm	(1) Layer thickness = 0.25 mm (Highest) (2) Build orientation = 15° (3) Raster angle = 30° (4) Raster width = 0.5063 (Highest) Air gap = 0.004 mm	3.046
Stephen O. Akande	2015	[122]	Factorial design, Pareto chart, DFA	PLA	Not reported	(1) Layer thickness = 0.25, 0.50 mm (2) Print speed = 16, 21.33 mm/s Infill density = 20%, 100%	(1) Layer thickness = 0.25 mm (Lowest) (2) Print speed = 16 mm/s (Lowest) Infill density = 20% (Lowest)	2.46
Vijay.B.Nidagundi	2015	[46]	Taguchi's L9 orthogonal array, Main effect plot of S/N ratio, ANOVA	ABS	Not reported	(1) Layer thickness = 0.10, 0.20, 0.30 mm (2) Build orientation = 0, 15, 30 (3) Fill angle = 0, 30, 60	(1) Layer thickness = 0.1 mm (Lowest) (2) Build orientation = 0 (Lowest) (3) Fill angle = 0 (Lowest)	0.3410
Francesca Chaidas	2016	[123]	Direct experimental effect	PLA	Not reported	(1) Contour width = 1, 2, 3 mm Extrusion temp = 210, 220, 230 °C	(1) Contour width = 2 mm (2) Extrusion temp = 230 °C (Highest)	12.84
Kishore	2018	[124]	ANOVA, Multiple Regression Analysis	PLA	Not reported	(1) Layer thickness = 0.06, 0.08, 0.10, 0.12 mm (2) Build orientation = 0, 45, 60, 90° (3) Infill density = 20, 30, 40, 50%	(1) Layer thickness = 0.12 mm (Highest) (2) Build orientation = 45° (3) Infill density = 40%	2.25
Kovan	2018	[125]	Direct experimental effect	PLA	(1) Print speed = 60 mm/s (2) Bed temp = 65 °C (3) Infill density = 35%	(1) Layer thickness = 0.10, 0.20, 0.40 mm (2) Extrusion temp = 190, 210, 230 °C	(1) Layer thickness = 0.10 mm (Lowest) (2) Extrusion temp = 210 °C	7.8
Velineni	2018	[126]	Full factorial design, ANOVA, Pareto	PLA	(1) Extrusion temp = 260	(1) Layer thickness = 0.1, 0.2, 0.3 mm	(1) Layer thickness =	6.12-7.22

			chart, Main effect and interaction plots, Control chart, Capability histogram		°C	(2) Print speed = 60, 80, 100 (3) Build orientation = 0, 45, 90	0.10mm (Lowest) (2) Print speed = 80 mm/s (3) Build orientation = 0	
Vinaykumar S Jatti	2019	[127]	Direct experimental effect	PLA	(1) Nozzle diameter = 0.4 mm	(1) Infill density = 10,33,55,78,100% (2) Print speed = 20,35,50,65,80 mm/s (3) Layer thickness = 0.08,0.16,0.24,0.32,0.40 mm (4) Extrusion temp = 190,200,210,220,230 °C	(1) Infill density =55% (2) Print speed = 20 mm/s (3) Layer thickness = 0.08 mm (4) Extrusion temp = 210 °C *Infill density, print speed and extrusion temp less effect*	10
Mishra	2019	[128]	Taguchi L27 Orthogonal, ANOVA, S/N ratio, regression analysis	ABS	Post-processing = Chemical treatment	(1) Raster angle = 0, 45, 90 (2) Raster width = 0.3556, 0.5306, 0.7306 mm Air gap = 0, 0.05, 0.10 mm	(1) Raster angle = 37 (2) Raster width = 0.5102 mm Air gap = 0.02 mm	5.74
Jiangchou Jiang	2019	[129]	Direct experimental effect	PLA	(1) Layer thickness = 0.20 mm (2) Shell thickness = 0.80 mm (3) Fill density = 0% (4) No support types Print speed = 30 mm/s	(1) Overhang angle = 20, 30, 40, 50° (2) Extrusion temperature = 175, 190, 205, 220 °C	(1) Overhang angle = 50° (2) Extrusion temperature = 175 °C	0.057
Yunus	2020	[130]	Direct experimental effect	ABS+ P430	(1) Infill density = 60% (2) Infill pattern = crossed ± 450 (3) Layer thickness = 0.10 mm (4) Nozzle diameter = 0.60 mm	(1) Raster angle = 0, 15, 30, 45, 60, 75, 90 (2) Build orientation = Horizontal, Vertical, Perpendicular	(1) Raster angle = 0 (Lowest) (2) Build orientation = Vertical	3-9
Sammaiah	2020	[131]	Direct experimental effect	ABS	(1) Extrusion temperature = 265 °C (2) Bed temperature = 150 °C	(1) Infill density = 20, 40, 60, 80, 100 (2) Layer thickness = 0.06, 0.1, 0.14, 0.18, 0.22, 0.26 mm	(1) Infill density = 20% (Lowest) (2) Layer thickness = 0.06 mm (Lowest)	2.16
M Sumalatha	2021	[132]	Taguchi L9 orthogonal, ANOVA, S/N ratio	ABS	Extrusion temperature = 230 °C	(1) Print speed = 40, 55, 70 mm/s (2) Layer thickness =0.2, 0.3, 0.4 mm (3) Infill density = 25, 33, 50	(1) Print speed = 40 mm/s (Lowest) (2) Layer thickness = 0.4 mm (Highest) (3) Infill density = 50 (Highest)	6.24
Jasgurpreet Singh Chohan	2022	[49]	Taguchi L9 orthogonal, ANOVA, S/N ratio	ABS	Layer thickness = 0.1 mm	(1) Extrusion temperature = 210, 230, 250 (2) Print speed = 60, 70,	(1) Extrusion temperature = 210 °C	1.50

80 (3) Infill pattern= Lines, Triangles, Tetrahedral	(Lowest) (2) Print speed = 70 mm/s (Middle) (3) Infill pattern = Triangles

DFA: Desirability function analysis; RSM: response surface methodology; GRA: grey relational analysis; RSM: response surface methodology.

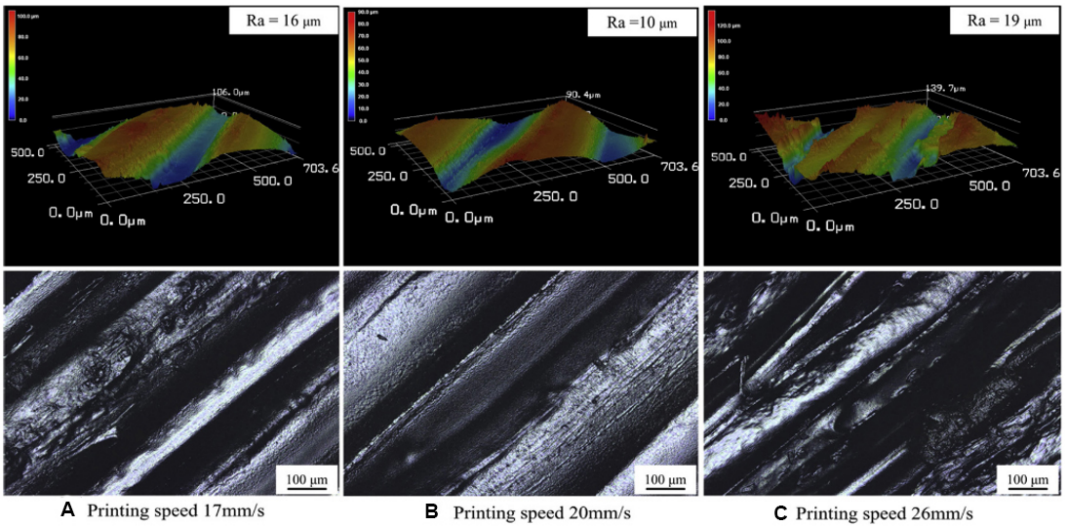

Figure 8. Surface topography in horizontal direction of PEEK parts printed using a Ø0.4 mm nozzle under different printing speeds, reproduced with permission[44], Copyright 2019 Elsevier.

surface has a better surface finish compared to the side of the printed part. To reduce the overall surface roughness, printing the shortest part in the Z-direction is recommended. Furthermore, a low print speed and extrusion temperature are preferable to achieve good surface quality. In the work of Chohan *et al.* the authors reported that printing speed has a higher influencing factor with an 83.41% contribution on surface quality compared with the extrusion temperature (9.04%)[49]. The extrusion temperature should be set below its glass transition temperature. High extrusion temperatures cause the viscosity of filament materials to increase, i.e., they become more fluid, resulting in increased dimensional deviation and surface roughness. The raster angle and air gap have less impact on surface quality, as confirmed by Kumar *et al.*[50]. However, in contrast, there was a contractionary statement from Sukindar *et al.* who discovered that the raster angle has a significant influence on surface roughness[51]. A zeroair gap is preferable to achieve good surface quality. Contour width did not have much influence on the surface finish on surface roughness.

To manufacture precise parts with critical dimensions, the surface roughness should be to equal or less than 0.8 μm. The surface roughness for FDM-printed parts without post-treatment ranges from 4 to 5 μm on average for Acrylonitrile Butadiene Styrene (ABS) and Polylactic acid (PLA). Based on a literature review, their maximum surface roughness for FDM-printed parts was 12 μm. Thus, for a surface quality enhancement in additive manufacturing, researchers have intensively explored various techniques for treatment. The roughness values recorded greatly decreased, with a reduction of up to 95%[52].

Mechanical strength

The strength of a printed product is defined as the ability to withstand the forces without deformation. Depending on the application areas, mechanical characteristics can be used as guidelines to explore new

application areas and determine the capability to replace the conventional parts or the expected service life of a part. The mechanical properties of FDM-printed parts are decreased compared with their raw filament material properties due to the heating-cooling process. In general, the mechanical properties of FDM-printed parts can be examined using ASTM standards. Table 2 shows a summary of research studies that have investigated the key parameters that influence the mechanical-related strength, including tensile, compression, flexural and impact strength. Tensile strength (ASTM D638), compressive strength and flexural strength (ASTM D790) were the three most widely analyzed mechanical properties of FDM parts. After the sample is fabricated, testing is carried out according to the standard process until the component ruptures and the load-strain relationship for each part is calculated. This relationship allows the determination and further analysis of the mechanical properties that are required for a specific application. The key parameters that can contribute to mechanical strength are discussed below:

a. Effect of layer thickness on mechanical strength: Tensile strength decreases with increasing layer thickness for both PLA and ABS filaments. Abbas *et al.* believed that the smallest layer thickness greatly enhanced the printed part strength because excellent interlayer bonding adhesion with less microvoids was generated at the smaller layer thickness[53]. Coogan *et al.* reported a large contact area (bonding width) for a low layer thickness that had an oval shape because of the wetting and better fusing of the filament [Figure 9][54]. A higher elastic modulus and yield stress are observed for a lower layer thickness[55]. Some researchers have found that as the layer thickness increases, the tensile and flexural strength also increase[56,57]. The authors believed that a smaller number of layers is needed because they depend on the mechanical adhesion bonding between layers. Wu *et al.* reported that the tensile strength increased with layer thickness increments from 200 to 300 μm[58]; however, the strength was reduced at a layer thickness of 400 μm. This phenomenon occurred as a result of a weak interlayer caused by shrinkage and delamination of the welded layer, while residue stress was present among the stacking beads as a result of the temperature variation between the new molten layer and the previous solidified layer, resulting in strength degradation. While a smaller layer thickness is beneficial for tensile strength, this is not the case for compressive and impact loadings. The impact resistance and compressive strength of parts were found to have a direct relationship with the layer thickness.

Sharma *et al.* found that increasing the layer thickness from 0.1 to 0.3 mm resulted in an increase of the compressive stress from 33 to 42 MPa[59]. This was attributed to the fact that during the compression testing, a number of layers are prone to slide over each other due to shear stress causing the specimen to fail. For impact strength, which is defined as the ability of a material to absorb shock loads without breaking, greater bonding is required to absorb or transfer the stress between the microstructure of a layer. The impact resistance of the part decreased with a reduction in the layer thickness. This finding is in agreement with the results of Ramkumar *et al.* Hardness is defined as the ability to resist any deformation under concentration force and it decreases with each increment of layer thickness[60]. A high layer thickness produces a lower number of printed layers, which provides weaker bonder strength compared to the low layer thickness with a large number of printed layers. The temperature gradient in the initial layers increases as the number of layers increases. This causes the diffusion process between neighboring rasters to increase, thereby lowering the void ratio and strengthening the bonding. However, this can also lead to a greater number of heating and cooling cycles and can therefore increase the residual stress.

b. Effect of infill density and pattern on mechanical strength: The mechanical strength increases with the increment of infill density. This is due to more material having been deposited and hence the density increases with less hollow space inside the part, meaning more force is required to deform or change its original shape. The direct relationship was observed in previous studies for flexural and tensile strength and

Ahmad *et al. Soft Sci* 2022;2:11 | https://dx.doi.org/10.20517/ss.2022.08

Table 2. Summary of research studies investigating the influence of key parameters on mechanical strength in FDM printing

First authors	Year	Reference	Method	Mat.	Fix item	Variable item	Optimum	Mechanical properties
Sandeep Raut	2014	[69]	Direct experimental effect	ABS	(1) With support material (0.05 and 0.13 in2) (2) Formula for cost calculation	(1) Build orientation = X (0, 45, 90°); Y (0, 45, 90°); Z (0, 45, 90°);	(1) Build orientation = X (0): good flexural strength and medium cost Y (0): good tensile strength and minimum cost	(1) Tensile strength = 33 - 35.45 MPa (2) Flexural strength = 28-45 MPa
Farzad Rayegani	2014	[133]	Full factorial, hybrid GMDH, and differential evolution (DE)	ABS P400	(1) Ambient temp = 23 °C (2) Humidity = 50%	(1) Build orientation = 0, 90° (2) Raster angle = 0, 45° (3) Raster width = 0.2034, 0.5588 mm (4) Air gap = -0.0025, 0.5588 mm	(1) Build orientation = 0° (Lowest) (2) Raster angle = 50° (Highest) (3) Raster width = 0.2034 mm (Lowest) (4) Air gap = -0.0025 mm (Lowest)	(1) Tensile strength = 36.86 MPa
Wenzheng Wu	2015	[58]	Direct experimental effect	PEEK and ABS	(1) Build orientation = Y direction (Flat) (2) Fill pattern = Line (3) Air gap = 0 (4) Number of contours = 2 (5) Nozzle diameter = 0.4 mm	(1) Layer thickness = 200, 300, 400 μm (2) Raster angle = 0/90, 30/60, 45/-45°	(1) Layer thickness = 300 mm (Medium) (2) Raster angle = 0/90° (Lowest)	(1) Tensile strength = 56.6 (2) Compression strength = 60.9 MPa (300 μm)
O.S. Carneiro	2015	[76]	Direct experimental effect	PP	(1) Extrusion temperature = 165 °C (2) Bed temperature = Room temperature (3) Print speed = 8 mm/s (1st layer); 60 mm/s (other layer)	(1) Infill density = 20, 60, 100% (2) Build orientation = 45, 0, 90, crossed 45 (±45) and crossed 0-90 (3) Layer thickness = 0.20 and 0.35 mm	(1) Infill density = 100% (Highest) (2) Build orientation = ±45 (3) Layer thickness = 0.20 mm (Lowest)	(1) Young Modulus = 1000 MPa (2) Ultimate tensile strength = 20 MPa
Vijay.B. Nidagundi	2015	[46]	Taguchi's L9 orthogonal array, Taguchi's S/N ratio, ANOVA	ABS	Not reported	(1) Layer thickness = 0.10, 0.20, 0.30 mm (2) Build orientation = 0, 15, 30 (3) Fill angle = 0, 30, 60	(1) Layer thickness = 0.1 mm (Lowest) (2) Build orientation = 0 (Lowest) (3) Infill angle = 0 (Lowest)	(1) Ultimate tensile strength = 28.1 N/mm^2 (2) Dimensional accuracy = 1024.8 mm^3 (3) Surface roughness = 0.3410 μm (4) Manufacturing time = 68 min (0.3 μm layer thickness)
Pritish Shubham	2016	[134]	Direct experimental effect	ABS	(1) Print speed = 15 mm/s Environment temp= 25 °C	(1) Layer thickness = 0.075, 0.10, 0.25, 0.50 mm	(1) Layer thickness = 0.075 mm (Lowest)	(1) Tensile strength = 27.5 MPa (Stress-strain curve) (2) Impact strength = 79.1 MPa
Z Z. Abdullah	2017	[78]	Two-way ANOVA, Main effect plot	ABS and PLA	(1) Build orientation = Flat (2) Air gap = Level 1 (3) Fill density/pattern = 30%, Rectilinear	(1) Layer thickness = 0.20, 0.30, 0.40 mm (2) Raster angle = 30/60, 45/-45, 0/90	(1) Layer thickness = 0.4 mm (PLA); 0.3mm (ABS) (2) Raster angle = 30°/60° (PLA); 45°/-45° (ABS)	(1) Tensile strength = 33 MPa (PLA); 24 MPa (ABS) (2) Flexural strength = 49 MPa (PLA); 35 MPa (ABS)

					(4) Extrusion temperature = 210 °C			
J.M. Chacón	2017	[135]	ANOVA analysis, regression models and response surfaces	PLA	(1) Air gap = 0 mm (2) Raster angle = 0° (3) Extrusion temp = 210 °C	(1) Build orientation = Flat (F), On-edge (O), Upright (U) (2) Layer thickness = 0.06, 0.12, 0.18, 0.24 mm (3) Extrusion speed rate = 20, 50, 80 mm/s	(1) Build orientation = Flat (2) Layer thickness = 0.06 mm (Lowest) (3) Extrusion speed rate = 80 mm/s (Highest)	(1) Tensile strength = 87 MPa (Flat; 0.06 mm layer thickness; 80 mm/s speed rate) (2) Flexural strength = 63 MPa (On edge; 0.06mm; 80mm/s speed rate)
Tahseen Fadhil Abbas	2018	[53]	Direct experimental effect	PLA	(1) Print speed = 100 mm/s (2) Infill density = 80% (3) Build orientation= 45°	(1) Layer thickness = 0.10, 0.15, 0.20, 0.25, 0.30 mm	(1) Layer thickness = 0.1 mm (Lowest)	(1) Impact strength= 16.7 KJ/m^2
Vladimir E. Kuznetsov	2018	[136]	Direct experimental effect	PLA	(1) Print speed = 25 mm/s	(1) Nozzle diameter = 0.40, 0.60, 0.80 mm (2) Layer thickness = 0.06- 0.60 mm	(1) Nozzle diameter = 0.4 mm (Lowest) (2) Layer thickness = 0.06 mm (Lowest)	(1) Flexural strength = 60-80 MPa
Claire Benwood	2018	[137]	Direct experimental effect	PLA	(1) Print speed = 50 mm/s (2) Infill density = 100% (3) Print time = 6.5 hours	(1) Bed temp = 45, 60, 75, 90, 105 °C (2) Extrusion temp = 190, 200,210, 220, 230 °C (3) Annealing temp = 80, 100 °C (4) Raster angle = 45/45, 30/60, 15/75, 0/90	(1) Bed temp = 105 °C (Highest) (2) Extrusion temp = 200 °C	(1) Tensile strength = 65 MPa (2) Flexural strength = 110 MPa
Martin Spoerk	2018	[138]	Direct experimental effect	PLA and ABS	(1) Print speed = 50 mm/min (2) Filament diameter = 1.75 mm	(1) Bed temperature= 30-120 °C (2) Bed material = Glass, PI	(1) Bed temp = 70 °C (PLA); 120 °C (ABS) (2) Bed material = Glass (PLA); PI (ABS)	(1) Adhesion force (Increase) (2) Contact angle (Reduce)
K.G. Jaya Christiyan	2018	[80]	ANOVA (quadratic model), Normal Probability plot, Contour plot, Response surface graph	PLA	(1) Fill pattern = -45/45 (2) Extrusion temperature = 180 °C (3) Bed temperature = 40 °C (4) Infill percentage = 70%	(1) Nozzle diameter = 0.40, 0.50, 0.60 mm (2) Layer thickness= 0.20, 0.25, 0.30 mm (3) Print speed = 30, 40, 50 mm/s	(1) Nozzle diameter = 0.40 mm (Lowest) (2) Layer thickness = 0.20 mm (Lowest) (3) Print speed = 40 mm/s (Medium)	(1) Flexural strength = 102.88 MPa
Łukasz Miazio	2019	[71]	Statistical analysis	PLA	(1) Extrusion temperature = 215 °C (2) Layer thickness = 0.2 mm (3) Fill density = 30%	(1) Print speed = 20, 30, 40, 50, 60, 70, 80, 90, 100 mm/s	(1) Print speed = 50-80 mm/s	(1) Breaking force = 0.55 kN
Ding	2019	[139]	Direct experimental effect	PEEK and PEI	(1) Bed temperature = 270 (PEEK), 210 (PEI) (2) Layer thickness = 0.2 mm (3) Print speed = 20 mm/s	(1) Extrusion temperature = 360, 370, 380, 390, 400, 410, 420 (2) Build orientation = Vertical, Horizontal	(1) Extrusion temperature = 390-400 °C for PEEK; 420 °C for PEI (2) Build orientation = Horizontal	(1) Flexural strength = 135 MPa (PEEK), and 123 MPa (PEI)
Vinaykumar S Jatti	2019	[127]	Direct experimental effect	PLA	(1) Nozzle diameter = 0.4 mm	(1) Infill density = 10, 33, 55, 78, 100% (2) Print speed = 20, 35, 50, 65, 80 mm/s	(1) Tensile strength = 58 N/mm^2 (Infill density = 100%, Print speed = 50 mm/s, Layer thickness = 0.16 mm, Extrusion temp = 220 °C) (2) Impact strength = 3.5	

					(3) Layer thickness = 0.08, 0.16, 0.24, 0.32, 0.4 mm (4) Extrusion temp= 190, 200, 210, 220, 230 °C	KJ/m^2 (Infill density = 55%, Print speed = 35 mm/s, 0.24 mm, Extrusion temp= 190 °C (3) Flexural strength = 70 N/mm^2 (Infill density = 100%, Print speed = 65 mm/s, Layer thickness = 0.24 mm, Extrusion temp = 230 °C)	
Sunil Khabia	2020 [140]	Direct experimental effect	Z-ABS, ABS	(1) Nozzle diameter = 0.40 mm	(1) Layer thickness = 0.09, 0.14, 0.19, 0.29, 0.39 mm	(1) Layer thickness = 0.09 mm (Lowest)	(1) Tensile stress = 30.2 MPa (2) Tensile elongation at maximum load = 3.07994 mm (3) Tensile elongation at break = 7.61126 mm (4) Tensile strength = 30.2 MPa
Praveen Kumar Nayak	2020 [141]	Direct experimental effect	ABS	Not reported	(1) Layer thickness = 0.178, 0.254, 0.330 mm (2) Build orientation = 0, 15, 30°	(1) Layer thickness = 0.33 mm (Highest) (2) Build orientation = 0 (Lowest)	(1) Tensile strength = 53.1 MPa
Yachen Zhao	2020 [142]	Direct experimental effect	PEEK	(1) Layer thickness = 0.15 mm (2) Print speed = 60 mm/s (3) Nozzle diameter = 0.40 mm (4) Line spacing = 0.40 mm	(1) Raster angle= 0°, 45° and 90° (2) Extrusion temp = 360, 380, 400, 420 °C (3) Ambient temp = 50, 65, 80 °C (4) Post treatment temp= 20 °C (room temp), 150 °C, 175°C, 200 °C, 225 °C, 250 °C	(1) Raster angle = 0 (Lowest) (2) Extrusion temp = 400 °C (High) (3) Ambient temp = 80 °C (Highest) (4) Post treatment temp = 250 °C (Highest)	(1) Tensile strength = 95.4 MPa
Valean	2020 [143]	Direct experimental effect	PLA	Not reported	(1) Build orientation = 0°, 45° and 90° (2) Layer thickness = 1.25, 2.15, 3.70, 8.00 mm	(1) Build orientation = 0 (Lowest) (2) Layer thickness = 1.25 mm (Lowest)	(1) Tensile strength =50.88 MPa
Yadav	2020 [144]	Direct experimental effect	ABS	(1) Layer thickness = 50-400 µm	(1) Build orientation = 0°, 45° and 90° (2) Infill pattern= Rectilinear, Gyroid	(1) Build orientation = 0 (2) Infill pattern = rectilinear for compression; gyroid for flexural strength	(1) Compression strength= 24.47 MPa (2) Flexural strength = 45.39 MPa
Hasçelik	2021 [81]	Direct experimental effect	Nylon	(1) Infill percentage = 100% (2) Layer thickness = 0.2 mm (3) Print speed = 45 mm/s (4) Bed temperature = 80 °C	(1) Extrusion temperature = 235, 240, 250, 260 °C (2) Raster angle = ±45, ± 45/0/90, 0/90, ±45/0/90	(1) Extrusion temperature = 260 °C (Highest) (2) Raster angle = ±45°	(1) Ultimate tensile strength = 40.2 MPa

PLA: Polylactic acid; ABS: acrylonitrile butadiene styrene; PET: polyethylene terephthalate; nylon: polyamide; PP: polypropylene.

impact resistance[60-62]. Vicente *et al.* reported that the tensile strength for the ABS-printed product increased from 700 to 720 MPa when the infill percent was increased from 95% to 105% (negative airgap)[63]. Apart from the infill density, the infill pattern also plays a role in the enhancement of the mechanical properties of the printed part as it influences the interaction between infilled filaments with one another. Alayoldi *et al.* reported no significant difference in

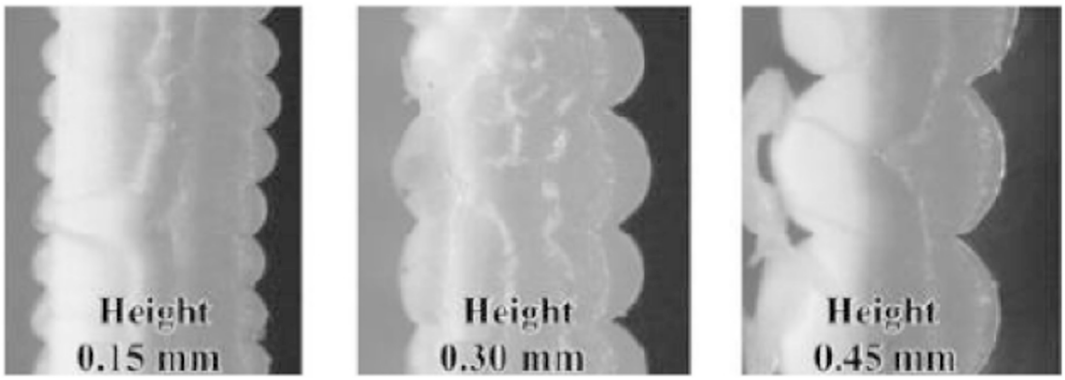

Figure 9. Contact area with increasing layer thickness, reproduced with permission[54], Copyright 2017 Emerald Publishing Limited.

tensile strength between triangular (66.3 MPa), grid (72.0 MPa) and hexagonal (58.8 MPa) infilled patterns[64]; however, the quarter cubic exhibited a lower strength of 27.4 MPa. This is due to the grid pattern having a special layer arrangement where the layers crisscross above each other, while the quarter cubic pattern has an offset between the layers [Figure 10].

c. Effect of build orientation on mechanical strength: In terms of the tensile strength of FDM-printed parts, most research shows that lower values (0°) of build orientation are best, whereas the flexural and impact strength properties show varied optimal orientations. However, it is subject to the direction of the load applied and the material properties[65]. Abdelrhman *et al.* reported a maximum tensile strength of 29.36 MPa and fracture load of 1409.09 N using an XY build orientation[66]. Eryildiz *et al.* reported 36% less tensile strength for an upright orientation (35.52 MPa) compared to the flat 0° orientation (55.49 MPa) because of the fracture mode and loading direction[67]. The interlayer fracture strength mainly depends on the interlayer bonding strength, while the intralayer fracture mainly depends on the strength of the extruded material [Figure 11A]. Vishwas *et al.* found that the tensile strength was maximized for ABS-printed parts (26.41 MPa) using a 15° orientation and using a 30° build orientation for nylon (25.48 MPa)[68]. Raut *et al.* reported that the lowest build orientation is optimal for the tensile strength of ABS parts (35.45 MPa at x axes |22.51 MPa at y axes|33.00 MPa at z axes)[69]. In the case of the flexural strength, the higher build orientation levels resulted in better flexural strength values, excluding the x axis. The maximum flexural strength of 45.20 MPa was noted using the 0° build orientation with respect to the x axis. The illustration of the relationship between the tensile and flexural strength of ABS parts and different build orientation levels with respect to the x, y and z axes is shown in Figure 11B.

d. Effect of print speed on mechanical strength: Some researchers have highlighted that print speed has a significant influence on mechanical strength[70], while others have reported that it is almost unaffected. As a result, strength is determined by layer-to-layer adhesion. Miazio *et al.* investigated the relationship between print speed, which varied from 20 to 100 mm/s, with tensile strength[71]. The authors reported no significant difference for the print speed range of 50-80 mm/s; however, after 80 mm/s, the strength was decreased. This is caused by the limited capacity of the print head. The time needed to plasticize the filament is too short. In turn, the printing time exponentially increases with a decrease in speed. For high speed printing, less material is deposited, leading to void formation that reduces the overall strength of the printed part.

e. Effect of extrusion temperature on mechanical strength: The strength-extrusion temperature relationship is not linear. Tensile and flexural strength increase with extrusion temperature until they reach a maximum value and start to deteriorate when exceeding the glass transition temperature. When an extrusion

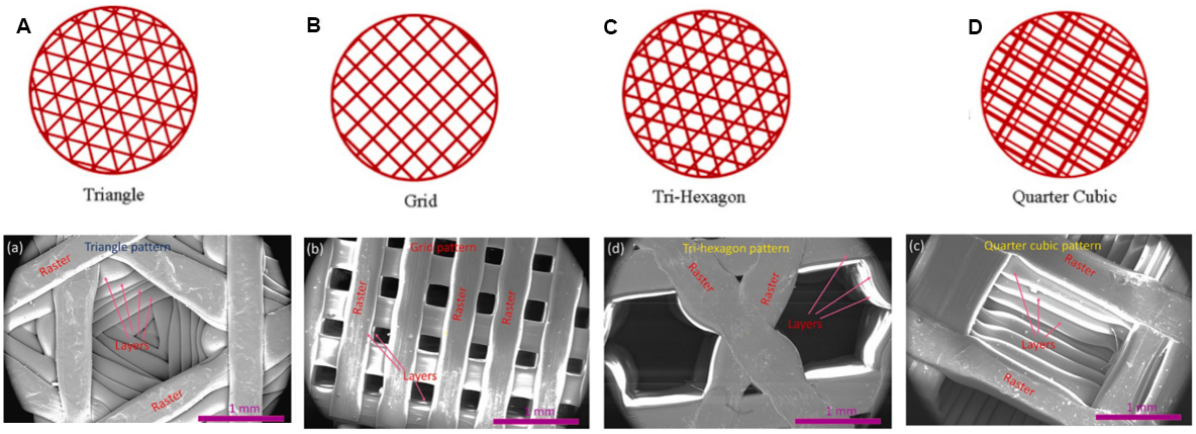

Figure 10. Illustration and SEM images of 3D printed specimens at different infill patterns: (A) triangle; (B) grid; (C) tri-hexagon; (D) quarter cube patterns, reproduced with permission[64], Copyright 2020 Elsevier.

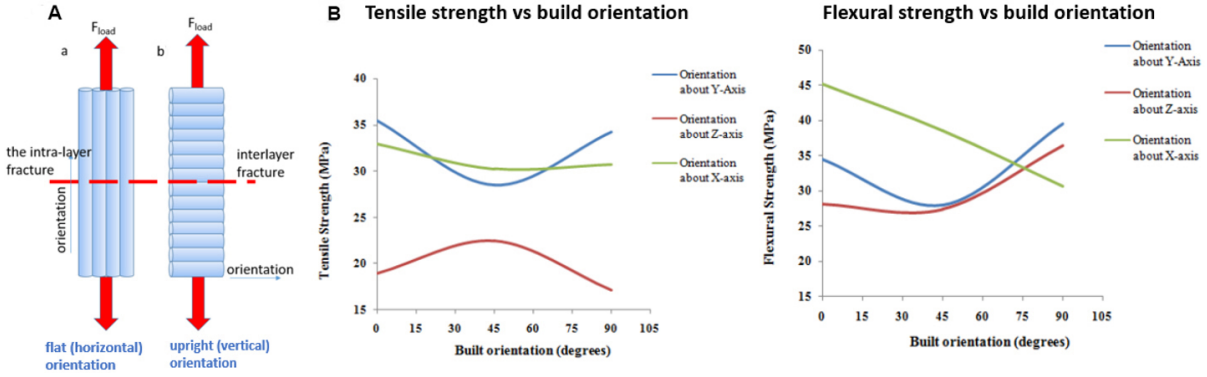

Figure 11. (A) Tensile failure mechanism, reproduced with permission[67]. Copyright 2021 Europe Mechanical Science; (B) relationship of tensile and flexural strength against build orientation, reproduced with permission[69], Copyright 2014 Elsevier.

temperature is below the filament material's glass transition temperature, the new layer fuses with the extruded layer and interlayer bonding is generated. High extrusion temperatures above the glass transition temperature provide strong interlayer bonding between layers and the oval bead shape is created, resulting in an increment of strength. However, some researchers believe that as the temperature increases[72], the viscosity of the filament material reduces, resulting in a reduction in the overall thickness of the part that can lead to strength degradation. The material also tends to undergo degradation[73] and becomes more brittle at high temperatures [Figure 12][74]. In order to increase the bonding between layers, the diffusion time, which refers to the time taken for the material to cool down to its glass transition temperature, should be increased. Zhou *et al.* concluded that an increase in extrusion and bed temperature extends the diffusion time, resulting in increased bond strength and overall mechanical properties[75].

f. Effect of raster related parameter on mechanical strength: It was reported that the minimum level (0°) of raster angle improves the tensile and flexural strength of FDM parts, while the impact strength can be improved using a 45°/-45° (staggered raster) raster angle. In fact, the strength relies on the direction of the load applied[76] as the molecules tend to align along the stress axis direction. The tensile strength decreases as the raster angle increases. 0° raster angle is the optimal level in terms of tensile strength along with a 0.1 mm layer thickness and 0° part orientation. This is because tensile strength depends on the alignment between

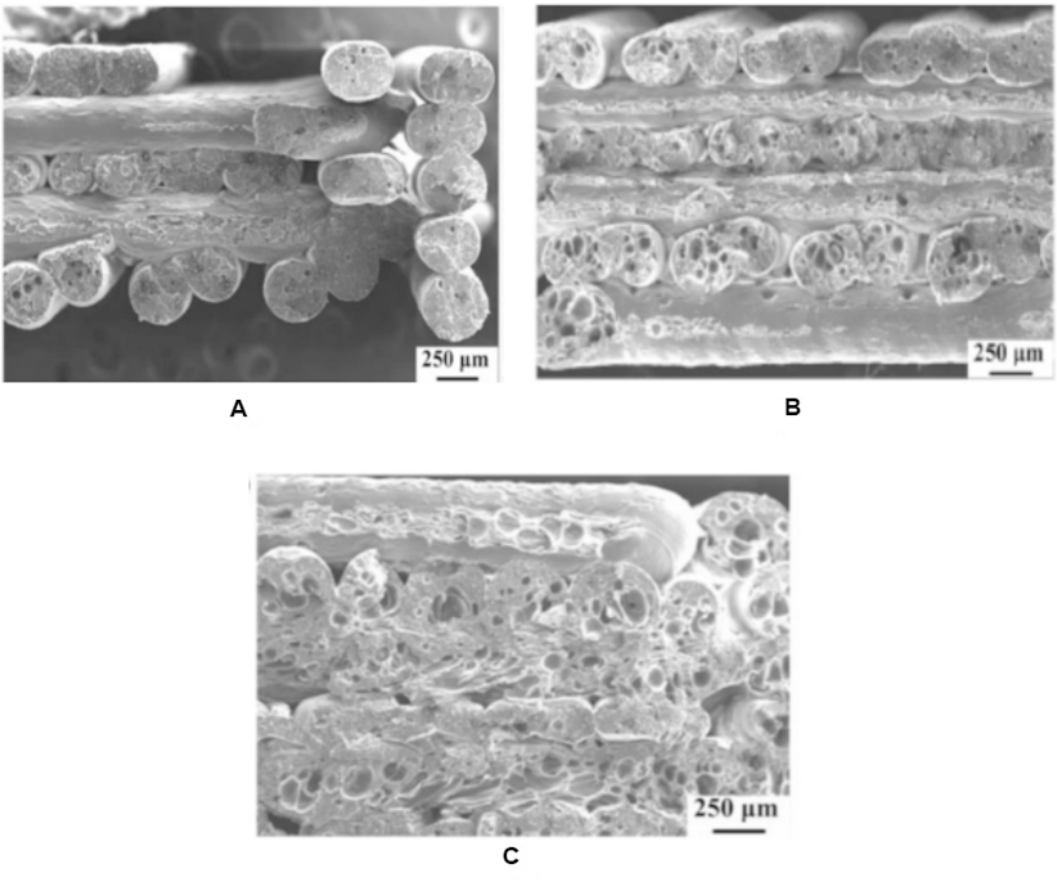

Figure 12. SEM images of fracture surfaces printed at different temperatures: (A) 200; (B) 220; (C) 240 °C, reproduced with permission[74], Copyright 2021 MDPI.

the axis where the stress is applied. Therefore, increasing the raster angle results in a misalignment between two axes causing weaker parts in terms of tensile strength. In the case of a PLA resin, Liu *et al.* found that the raster angle of 0° is optimal and results in the highest tensile and flexural strength[77]. The authors studied three levels of raster angle, namely, long-raster (0°), long-short-raster (+90°/0°) and staggered-raster (+45°/-45°). The long-short-raster means a layer with a 90° raster angle is followed by a consecutive layer with a 0° raster angle during the printing process. Based on the results of ANOVA analysis that demonstrates the percentage contribution of parameters, it was found that the raster angle parameter mostly affects the impact strength (0.127%) of PLA parts compared to tensile (0.002%) and flexural strength (0.034%). The optimal level in terms of the impact strength was found to be staggered-raster (+45°/-45°).

g. Short discussion and summary of key parameters related to mechanical strength: For tensile properties, the build orientation and layer thickness were found to be the most significant parameters in achieving maximum tensile strength. Lower values (0°) of build orientation and layer thickness are recommended for tensile strength. According to Abdullah *et al.* layer thickness and raster angle have a significant impact on tensile strength in isolation but not in combination[78]. Although the optimum raster orientation for tensile strength is still contradictory, it may be concluded that a 0°/90° or -45°/45° raster orientation is optimum. Rao *et al.* reported that the extrusion temperature and infill pattern contributed 7.95% and 3.93% to tensile strength in their study[79]. Tensile strength increases in a non-linear relationship with extrusion temperature, whereas it increases until it reaches maximum value and begins to deteriorate. High extrusion temperature

and below the glass transition temperature is preferable for tensile strength. However, extrusion temperatures did not have a significant influence as a printing speed parameter. The recommended print speed range is ~45-50 mm/s. The tensile strength is maximized at a high infill percentage and an infill pattern that has a layer arrangement that is crisscrossed with good intralayer bond connection.

For compressive properties, according to the state-of-art research, there are still very limited studies that investigate their relationship with process parameters that have been carried out. In our opinion, we believe further investigation is required to reach a solid conclusion on the process parameter relationship with compressive strength. For flexural properties, their relationship is more complex compared to tensile and compression strength as it involves both forces. The build orientation and layer thickness were found to be the most significant influence parameters on flexural strength. A 0° build orientation and low layer thickness are the optimum conditions to obtain the maximum flexural strength. According to Christiyan *et al*. the layer thickness influence was 36.61%, followed by nozzle diameter (27.45%) and print speed (5.39%) on flexural strength[80]. A high extrusion temperature is recommended to increase the flexural strength. Based on the current literature review, very little research has been conducted on other process parameters, such as the infill pattern and density, print speed and raster angle. It would be beneficial for public knowledge if researchers could explore more parameters to be analyzed concurrently to determine the influence of printed components on flexural strength as one of the future research directions.

Based on a literature review, the FDM-printed part of PEEK has superior properties, including tensile and flexural strength. The greatest tensile strength ranged from 56 to 95 MPa, followed by PLA (33-87 MPa), nylon (40.2 MPa), ABS (24-56.6 MPa) and PP (20 MPa). The highest flexural strength of 135 MPa was followed by PEI (123 MPa), PLA (49-110 MPa) and ABS (35-45 MPa). The mechanical properties after printing are decreased compared with their material properties in raw filament form and the comparison among various materials for before and after FDM printing is shown in Figure 13. The mechanical properties that should be targeted based on their application. Despite this, there is very little information available on the minimum value of mechanical properties that were required. From the existing research, it can be initially concluded that the intended tensile strength was ≥ 40 MPa[81] and the flexural strength was ≥ 214 MPa[82] to produce printed parts that dealt with heavy loads, such as load bearing. The intended compression strength was ≥ 24 MPa and the flexural strength was ≥ 45 MPa for products that did not deal with heavy loads.

Dimensional accuracy

Accuracy is defined as the difference[83] between the dimensions of a printed product and a virtual CAD model, which may differ due to material shrinkage[84] during the phase transition[85] or material expansion due to imperfect first layer adhesion[86] caused by the thermal gradient, resulting in warping. In this section, the key parameters that can influence the dimensional accuracy of the printed parts are summarized systematically in Table 3 and detailed explanations for each parameter are presented as follows:

a. Effect of layer thickness on dimensional accuracy: Thermoplastic materials have the issue of shrinkage when dealing with high and low temperatures. The dimensional accuracy is optimum for low layer thicknesses. However, there is a contradiction in this statement based on the findings of Sood *et al.* who recommended a high layer thickness as the optimum condition for dimensional accuracy[87]. This conflict can be narrowed down to the type of material as Sood *et al.* used PLA while Nancharaiah *et al.* and Milde *et al* used ABS for their studies[87-89]. ABS has a higher shrinkage rate compared to PLA. Material dependency is a considerable condition of the optimal layer thickness for selection that might affect dimensional accuracy. Basically, the nozzle extrudes the material onto a platform in an elliptical bead shape,

Table 3. Summary of research studies investigating the influence of key parameters on dimensional accuracy in FDM printing

First authors	Year	Reference	Methodology	Material used	Fix parameter	Variable item	Optimum value	Dimensional accuracy
Vijay. B. Nidagundi	2015	[46]	Taguchi L9 orthogonal array, Taguchi's S/N ratio, ANOVA	ABS	Not reported	(1) Layer thickness = 0.10, 0.20, 0.30 mm (2) Build orientation = 0, 15, 30 (3) Fill angle = 0, 30, 60	(1) Layer thickness = 0.10 mm (Lowest) (2) Build orientation = 0 (Lowest) (3) Fill angle = 0 (Lowest)	Dimensional for printed model (1036.05 mm^3) bigger than CAD model (1000 mm^3)
Stephen O. Akande	2015	[122]	Factorial design, Pareto chart, DFA	PLA	Not reported	(1) Layer thickness = 0.25, 0.50 mm (2) Print speed = 16, 21.33 mm/s (3) Infill density = 20%, 100%	(1) Layer thickness = 0.25 mm (Lowest) (2) Print speed = 16 mm/s (Lowest) (3) Infill density = 20% (Lowest)	The thickness dimension was the most inaccurate
Young-Hyu Choi	2016	[96]	Direct experimental effect	ABS	(1) Nozzle diameter = 0.8 mm (2) Extrusion temperature = 240 °C (3) Print speed = 50 mm/s (4) Layer height = 0.30 mm	(1) Bed temp = 40, 50, 70, 90, 110 °C	(1) Bed temp = 110 °C (Highest)	Heat shrinkage shape error (%) failed in AM at bed temp 40 °C
Ján Milde	2017	[89]	Arithmetical means	ABS	Not reported	(1) Layer thickness = 90, 190, 290 μm	(1) Layer thickness = 0.09 mm (Lowest)	Arithmetical mean deviation of -0.25 mm for 0.09 mm layer thickness
Saroj Kumar Padhi	2017	[102]	Taguchi L27 orthogonal array, fuzzy inference	ABS	Not reported	(1) Layer thickness = 0.127, 0.178, 0.254 mm (2) Build orientation = 0, 15, 30 (3) Raster angle = 0, 30, 60 (4) Raster width = 0.406, 0.456, 0.506 mm (5) Air gap = 0, 0.004, 0.008 mm	(1) Layer thickness = 0.178 mm (Medium) (2) Build orientation = 0° (Lowest) (3) Raster angle = 0° (Lowest) (4) Raster width = 0.4564 mm (Medium) (5) Air gap = 0.008 mm (Highest)	Layer thickness major contribution individually on L and T.
Ala'aldin Alafaghani	2017	[57]	Direct experimental effect	PLA	Not reported	(1) Build orientation = X, Y, Z (2) Infill density = 20, 50, 80% (3) Print speed = 70, 120, 170 mm/s (4) Extrusion temp = 175, 180, 205 °C (5) Layer thickness = 0.10, 0.25, 0.40 mm (6) Infill	(1) Build orientation = Z (2) Infill density = 50% (Medium) (3) Print speed = 90 mm/s (4) Extrusion temp = 185 °C (5) Layer thickness = 0.25 mm (Medium) (6) Infill pattern = Diamond F	The length of printed part smaller than model, while width and thickness dimensions increase

						pattern = Diamond F, Diamond, Linear, Hexagonal		
Vishwas M	2018	[68]	Taguchi Orthogonal Array	ABS	(1) Nozzle diameter = 0.40 mm (2) Filament diameter = 1.75 mm	(1) Layer thickness = 0.10, 0.20, 0.30 mm (2) Build orientation = 0, 15, 30 (3) Shell thickness = 0.4, 0.8, 1.2 mm	(1) Layer thickness = 0.30 mm (Highest) (2) Build orientation = 30 (Highest) (3) Shell thickness = 0.8 mm (Medium)	Dimensional for printed model (1007 mm^3) slightly bigger than CAD model (1000 mm^3)
				Nylon			(1) Layer thickness = 0.30 mm (Highest) (2) Build orientation = 15 (Medium (3) Shell thickness = 0.4 mm (Lowest)	Dimensional for printed model (1167.63 mm^3) bigger than CAD model (1000 mm^3)
Aissa Ouballouch	2019	[145]	Direct experimental effect	GRPA; KRPA	(1) Build orientation = 45°	(1) Extrusion temp = 245, 255, 265 °C (2) Print speed = 50, 60, 70 mm/s (3) Layer thickness = 0.10, 0.15, 0.20 mm	(1) Extrusion temp = 255 °C (Medium) (2) Print speed = 60 mm/s (Medium) (3) Layer thickness = 0.15 mm (Medium)	Dimensional accuracy of KRPA is more affected by the printing parameters than GRPA
OM F Marwah	2019	[103]	Fractional factorial design (ANOVA, Pareto chart, Main Effects Plot)	ABS	Not reported	(1) Layer thickness = 0.20, 0.25, 0.30 mm (2) Extrusion temp = 230, 235, 240 °C (3) Print speed = 50, 55, 60 mm/s (4) Infill density = 20, 25, 30 (5) Bed temp = 90, 95, 100 °C	(1) Layer thickness = 0.25 mm (Medium) (2) Extrusion temp = 235 °C (Medium) (3) Print speed = 55 mm/s (Medium) (4) Infill density = 25% (Medium) (5) Bed temp = 100 °C (Highest)	Different between CAD and printed model is 2.56%
Elizabeth Azhikannickal	2019	[146]	RMS (root mean square) error	ABS	(1) Extrusion temp = 230 °C	(1) Layer thickness = 0.10, 0.20, 0.34, 0.40 mm (2) Infill density = 20, 50, 100%	(1) Layer thickness = 0.4 mm (Highest) (2) Infill density = 100% (Highest)	Printed model not adhere to the print bed and the molten plastic at layer thickness ≥ 0.4 mm. No significant different on infill relationship with dimensional accuracy
Amirah Azwani Rosli	2020	[99]	Direct experimental effect	ABS	(1) Extrusion temp = 240 °C	(1) Bed temp = 90, 100, 110 °C	(1) Bed temp = 110 °C (Highest)	Warpage decreased with increasing bed temperature; thick sample indicated lower shrinkage
Ahmed Elkaseer	2020	[93]	Taguchi L50 orthogonal array	PLA	(1) Bed temp = 60 °C (2) Infill pattern = 45 Rectilinear	(1) Infill density = 20, 50% (2) Layer thickness = 0.10, 0.15, 0.20, 0.25,	Optimization X direction (1) Infill density = 35% (2) Layer thickness = 0.11	Thin layers and high printing speeds reduce percentage error

0.30 mm (3) Printing speed = 20,40, 60, 80 mm/s (4) Extrusion temp = 190, 200, 210, 220 °C (5) Surface inclination angle =0, 45, 60, 75	mm (3) Printing speed = 40.7 mm/s (4) Extrusion temp = 216 °C (5) Surface inclination angle = 45° Optimization Z direction (1) Infill density = 47% (2) Layer thickness = 0.11 mm (3) Printing speed = 95.8 mm/s (4) Extrusion temp = 226 °C

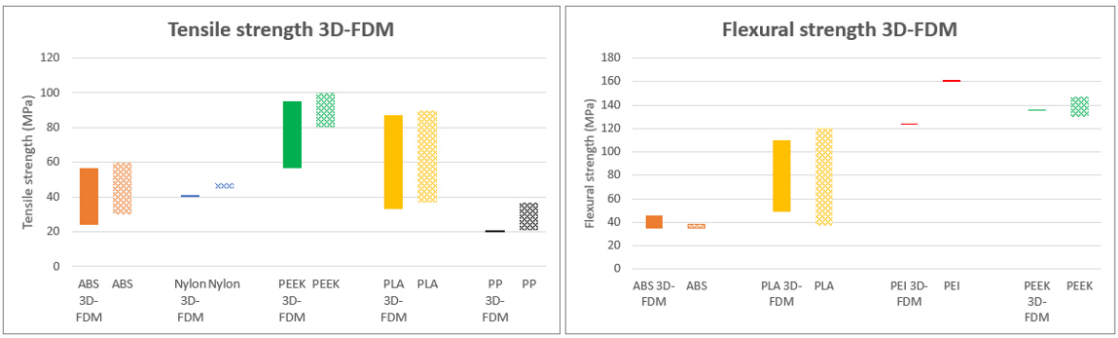

Figure 13. Comparison of tensile and flexural strength before and after printing among various materials (solid bar = after printing and strip bar = before printing).

which has an uneven surface. The next deposition will be stacked on the uneven previous layer, leading to dimensional variation, especially on the Z axis. Consideration of tolerance to compensate for shrinkage by scaling when printing is highly recommended in order to provide the ability to print the feature in the desired range of tolerance[90,91].

b. Effect of build orientation on dimensional accuracy: Deposition orientation in the Z-direction is the most significant parameter for dimensional accuracy. However, it is difficult to explain how building orientation can have an effect on dimensional accuracy. What is certain is that it clearly contributes to dimensional accuracy. There is the potential for printers to have differences in positional resolution. Attribution from gravity effects as it relates to a semi-liquid or liquid also has potential in this case. The 45° angle specimens had the lowest dimensional accuracy. This is because, due to layer positioning, there are expected to be layers of printed parts built tilted. As a result, the risk of distortion increases due to the gravity impact throughout curing[92].

c. Effect of extrusion temperature on dimensional accuracy: Depending on the printing material, it is important to set the extrusion temperature to the correct value. Too high extrusion temperatures (above the glass transition temperature) can degrade the surface quality. This might be explained by the increased extrusion temperature reducing the viscosity of the melted filament[93]. In other words, it will increase the fluidity of the extruded material, thereby allowing it to flow fast and out of control, thus contributing to

dimensional inaccuracy. This statement is agreed upon by most researchers[94,95].

d. Effect of bed temperature on dimensional accuracy: Warpage and shrinkage can be reduced with increasing bed temperature. Large differences between the extrusion and bed temperatures can cause a reduction in the ability to release the thermal stress and thus the heat shrinkage increases. Choi *et al.* highlighted that the bed temperature needs to be set as close as possible to the softening temperature of the filament material in order to compromise with a reduction in its heat shrinkage[96]. The lower shrinkage observed in the thick printed sample than the thin printed sample as thick printed sample might have a greater volume with a longer conduction path that causes a lower cooling rate that induces less thermal contraction[97]. Furthermore, it allows the printed part to not stick to the platform, which might generate the sticking mark and effect their dimensions[98].

e. Effect of infill density on dimensional accuracy: The infill density reflects the amount of filament material printed inside the object. The relationship between infill density and dimensional accuracy is not stated explicitly. The building parts need layers to support each other in order to reduce the potential for object collapse. Increased infill density allows for better dimensional control. In addition, the infill density determination also depends on the size of the printed parts. Due to the nature of the behavior of polymers that expand and shrink when dealing with heat, increased infill density increases the "fullness" amount of material inside the printed part, which means less space for them to expand or shrink, which has an effect on the dimensional accuracy. Rosli *et al.* highlighted that high-volume products (large size) have a low cooling rate, which causes less thermal contraction and contributes to lower shrinkage[99].

f. Effect of print speed on dimensional accuracy: In order to improve the dimensional accuracy, the print speed should be decreased. At high print speed, less material extrusion and time to connect the new molten state layer to the solidified layer reduce the dimensional accuracy. An unexpected result was observed in Agarwal *et al.* who found that the low print speed has higher dimensional deviation compared to the high print speed[100]. This is explained that once the shear rate exceeds a critical value, an increase in shear rate decreases the extrudate swell. In other words, higher print speeds increase the shear rate beyond a critical value after which the melted material on deposition does not flow.

g. Effect of air gap on dimensional accuracy: A positive or negative air gap spacing bring diffusion of the material between bead generate issue on dimensional tolerance because of over/underfilling at the contact area, which results in an uneven layer. As a result, the following layer deposited stacking on top of this uneven layer will not have an even planer surface, which might result in a dimension increase along the part construction direction[101].

h. Short discussion and summary of key parameters related to dimensional accuracy: The layer thickness is one of the most studied and significant parameters for dimensional accuracy according to the presented literature review. The setting of the optimum layer thickness is based on the material used to reflect the expansion-shrinkage rate once it has been dealt with heat. In contrast, a low layer thickness is recommended for easier dimension control. Nidagundi *et al.* highlighted that layer thickness has the greatest impact on the dimensional accuracy (75.52%), followed by build orientation (13.11%) and raster angle (11.67%)[46]. The same finding was found by Sood *et al.* Vishwas *et al.* highlighted that layer thickness gives the major contribution to dimensional accuracy (84.84%), followed by contour width or shell thickness (12.66%) and build orientation (2.5%)[68,87]. Sood *et al.* reported that layer thickness contributes 10.68%, 42.87% and 83.19% of the dimensional variation of the length (ΔL), width (ΔW) and thickness (ΔT), respectively[87]. Padhi *et al.* reported that layer thickness plays the main role in the dimensional variation of

ΔL and ΔT with 44.44% and 83.17%, respectively, while for ΔW dimensional accuracy, the main contributor parameter is build orientation (23.91%)[102]. Shrinkage was commonly noticed along the X and Y axes of build platforms, whereas expansion was observed along the Z axis of the build platform.

Marwah *et al*. disagreed that layer thickness is the main parameter that contributes to dimensional error[103]. They stated that the bed temperature has a greater influence on shrinkage than layer thickness, which was supported by ANOVA studies with a *P*-value of 0.000 when compared to the other four factors, which were layer thickness (*P*-value of 0.156), extrusion temperature (*P*-value of 0.595), print speed (*P*-value of 0.152) and infill density (*P*-value of 0.089). It is critical to adjust the extrusion temperature to the right value depending on the printing material. The authors highlighted that infill density is the highest impact parameter after extrusion temperature. Suaidi *et al*. reported that build orientation contributes 22.91%, layer thickness contributes 9.97% and infill density is 46.12%[104]. The significance of infill density was also found by Robles *et al*.[105]. Increased infill density allows for better dimensional control. However, the infill density finding conflicts with Alafaghani *et al*. finding as the authors highlighted that infill density and pattern have no or very little influence on the dimensional error[57]. In order to improve the dimensional accuracy, print speed should be decreased. According to their ANOVA analysis, Baraheni *et al*. reported that print speed has a significant effect on the dimensional error with a 43.92% contribution[106]. A zero air gap is recommended for minimal dimensional error.

However, in our perspective, further analysis is needed regarding the layer thickness, extrusion temperature, infill density, print speed and air gap for validation of the conclusion. The effects of many process parameters, including raster angle, raster width, number of shells and shell thickness, on dimensional accuracy are still unknown. To build a product with great dimensional precision, it is critical to understand the impact of these parameters. The need to have a very accurate dimensional printed part as close as possible to the original design is highly important as it will influence how well the product will be accepted and approved for distribution to the end users. Most research has focused on only two or three layers of parameters. It is highly recommended to analyze more than three levels of parameters and explore the effect of known parameters on dimensional accuracy in order to visualize their relationship, thereby leading to more accurate decisions. FDM printing should have a dimensional tolerance of ± 0.15% and a lower limit of ± 0.2 mm A tolerance of more than +/-0.5 mm is considered poor dimensional accuracy.

Based on the presented literature review, Figure 14 shows a summary of the fish-bone cause analysis, which consists of various FDM process parameters that influence the corresponding printed product characteristics (surface roughness, mechanical strength and dimensional accuracy) and their contribution rate. A simple summary of the relationship between the FDM process parameters and their output is depicted in Table 4 to better understand and identify the research gap in the key areas.

CHALLENGES

According to numerous research studies, it has been clearly identified that there are a few drawbacks that directly affect the part characteristics in FDM printed polymers that cannot be rectified solely by using the optimal printing conditions. Several significant challenges remain unresolved, which contribute to the part characteristics, including surface roughness, mechanical strength and dimensional accuracy. These are residual stresses caused by non-uniform temperature gradients, the existence of voids and the staircase effect.

a. Non-uniform heating and cooling cycles: In FDM, the internal stress increases in the printed part during the printing process due to rapid heating and cooling cycles, causing non-uniform temperature gradients

Table 4. Effect of design, process and material parameters for printed polymeric product

Aspect			Effect parameter			
Relationship effect			Surface roughness	Mechanical strength		Dimensional accuracy
				Tensile strength	Flexural strength	
Increment of key parameter						
Factor	Process perspective	Layer thickness	▲*	▼	-	▲*
		Infill density	▲	▲	▲	▲
		Air gap	▼	▼	-	▼
		Raster width	▼	▼	▲	-
		Raster angle	-	▲	-	-
		Build orientation	-	▼	-	▲*
		Print speed	▲	▼	▼	▼
		Extrusion temp	▼	▲	▲	▼
		Bed temp	-	-	-	▲

Definition: ▲= increase; ▼= decrease; ▲▼= increase then decrease; *other parameter dependent

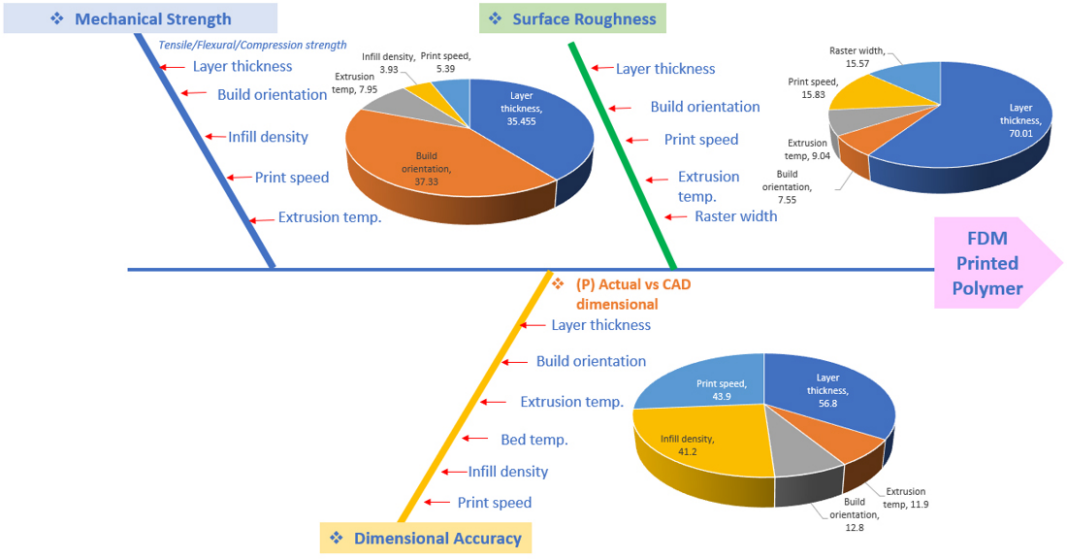

Figure 14. Cause analysis via a fish-bone diagram and contribution rate.

that lead to shape distortion, dimensional inaccuracy and inner layer cracking or delamination[107]. Non-uniform heating and cooling cycles are attributed to a number of factors, as follows: (1) conduction and forced convection release heat and the resulting drop in temperature, which drives the material to solidify fast onto the surrounding filaments. When the new extruded material is deposited on the previously solidified material and diffused in order to ensure the bonding is performed, a local re-melting is generated. This phenomenon leads to uneven heating and cooling and non-uniform temperature gradients being produced[108]. Thus, as a result, uneven stress affects the shape and dimensions of the printed part. Shrinkage, bucking, twisting and warpage are all examples of distortion defects that might be caused by this phenomenon, which involves the part lifting up and being unable to be placed properly on the printing platform; (2) the temperature gradient within a nozzle during the printing process has a significant effect on the print speed. The rate and amount of deposition material might affect the heating and cooling cycle, resulting in a different degree of thermal gradient on the printed part. The print speed is lower (faster) at lower layer thicknesses than at larger layer thicknesses. Shape distortion may be reduced by using the right

nozzle temperature, printing at a slower speed, and using a low layer thickness; (3) the design and size of the printed part have a significant effect on the thermal distribution, resulting in different stress and deformation behavior. At the bottom of the surface and each layer of printed part, the long raster tool-path exhibits a higher stress concentration pattern, and as each layer progresses, the stress accumulates at the initial deposition positions. To reduce tension, a short raster length is preferable along the long axis of the component; (4) high layer thickness, which means having a lesser number of layers, could reduce the accumulation of residual stress by reducing the number of heating and cooling cycles compared to the low layer thickness.

b. Existence of voids: A void is a small cavity that forms between the layers of a printed part. These voids weaken the part and make it prone to mechanical failure. They can cause delamination and the formation of porosity between subsequent layers, resulting in anisotropic characteristics. Stress concentrations formed at voids reduce part performance. Partial neck growth voids are a significant contributor to the occurrence of voids in FDM. The partial neck growth void occurs when there is incomplete neck growth between adjacent beads during the sintering process[109]. It is difficult to sustain neck growth with 100% coalescence between two adjacent beads[110]. Problems with solidification before complete coalescence may be caused by inherent characteristics, such as partial filling and inconsistent material flow[111]. The incomplete filling of the area inside the perimeter of the FDM part causes sub-perimeter voids. The travel direction of the extruder changes to a route that is tangent to the perimeter as the path approaches the perimeter. Thus, incomplete material flow for filling, which required sharper U-turns at these intersections, leads to void formation. Giving the perimeter a negative offset and/or raising the flow rate at the points of intersection are two methods for fixing this problem[112]. However, adjusting the process parameters should be done carefully to avoid the creation of new defects.

c. Staircase effect: To reduce surface roughness, we might use a low layer thickness. However, regardless of the low layer thickness, the inclined surface of FDM parts will always have a stair-stepping effect and the horizontal surface will always have a raster pattern. These visible rough patterns cannot be avoided, but surface finishing can be improved by using the best post-processing techniques. Surface quality improvement strategies are divided into two categories: mechanical and chemical. Some of the mechanical approach post-processing methods are manual sanding, gap filling, abrasive flow machining[113], abrasive milling[114], hot cutter machining, ball burnishing[115] and vibratory finishing. Example of chemical approaches are coating[116], acetone dipping and vapor smoothing. The manual post-processing method may become an issue in terms of labor costs and time, both of which are considerable on larger production volumes. The development of automated post-processing equipment by printer makers would help the industry expand its scope of applications and acceptance of additive manufacturing. There are numerous research studies focused on post processing for improving the surface quality of FDM parts[117-119]. They have discussed and assessed the best condition of post-processing techniques for improving the surface finish.

CONCLUSION AND FUTURE PERSPECTIVE

We are moving forward from a multi-step process to a single-step process with low-cost, low material wastage, high productivity and less production time. In this review, a list of process parameters with their definition, factors and effects on the characteristics of FDM-printed products, such as surface roughness, mechanical strength and dimensional accuracy, is presented. Layer thickness is the most influential factor on printed product quality among all FDM process parameters. There are still many unexplored factors that need further analysis. However, the study scope is limited to standard nozzle size and available software that attributes certain parameters such as layer thickness, raster width and number of outer shells. This constraint makes the optimization of variable process parameters more complex and needs to be overcome

by developing optimization techniques using statistical tools. Although numerous designs of experiments have been carried out to identify the relationships among parameters in terms of individual or combination parameter optimization studies for a single output variable, there are variations in the result findings. What is certain is that actual physical output differs from the prediction of optimization techniques. In the future, researchers must focus on multi-objective optimization to see concurrent relationships in multiple output variables. Hence, newer approaches to mathematical modeling might be required to synchronize and minimize the variation of the result. To achieve full acceptance, optimization must focus on meeting manufacturing requirements for reproducibility, reliability, precision, productivity, efficiency, manufacturing cost and balancing without jeopardizing one another. A clear and comprehensive understanding of their interrelations is necessary.

DECLARATIONS

Authors' contributions

Conceptualization, methodology, formal analysis, investigation, data curation, writing - original Draft: Ahmad NN

Validation, visualization, supervision, writing - review & editing: Ghazali NNN

Conceptualization, validation, resources, review & editing, visualization, supervision, project administration, funding acquisition: Wong YH

Availability of data and materials

Not applicable.

Financial support and sponsorship

This work was financially supported by "Skim Latihan Akademik Muda" (SLAM) from Universiti Teknologi Malaysia (UTM) and Impact-Oriented Interdisciplinary Research Grant Programme (IIRG018B-2019) from Universiti Malaya (UM).

Conflicts of interest

All authors declared that there are no conflicts of interest.

Ethical approval and consent to participate

Not applicable.

Consent for publication

Not applicable.

REFERENCES

1. Mohammed A, Elshaer A, Sareh P, Elsayed M, Hassanin H. Additive manufacturing technologies for drug delivery applications. *Int J Pharm* 2020;580:119245. DOI PubMed
2. Sheoran A, Kumar H. Fused deposition modeling process parameters optimization and effect on mechanical properties and part quality: review and reflection on present research. *Mater Today Proc* 2020;21:1659-72. DOI
3. Abdulhameed O, Al-ahmari A, Ameen W, Mian SH. Additive manufacturing: challenges, trends, and applications. *Adv Mech Eng* 2019;11:168781401882288. DOI
4. Daminabo S, Goel S, Grammatikos S, Nezhad H, Thakur V. Fused deposition modeling-based additive manufacturing (3D printing): techniques for polymer material systems. *Mater Today Chem* 2020;16:100248. DOI
5. Krieger KJ, Bertollo N, Dangol M, Sheridan JT, Lowery MM, O'Cearbhaill ED. Simple and customizable method for fabrication of high-aspect ratio microneedle molds using low-cost 3D printing. *Microsyst Nanoeng* 2019;5:42. DOI PubMed PMC

6. Dey A, Yodo N. A systematic survey of FDM process parameter optimization and their influence on part characteristics. *JMMP* 2019;3:64. DOI
7. Solomon IJ, Sevvel P, Gunasekaran J. A review on the various processing parameters in FDM. *Mater Today Proc* 2021;37:509-14. DOI
8. Zharylkassyn B, Perveen A, Talamona D. Effect of process parameters and materials on the dimensional accuracy of FDM parts. *Mater Today Proc* 2021;44:1307-11. DOI
9. Elkasabgy NA, Mahmoud AA, Maged A. 3D printing: an appealing route for customized drug delivery systems. *Int J Pharm* 2020;588:119732. DOI PubMed
10. Casavola C, Cazzato A, Moramarco V, Pappalettere C. Orthotropic mechanical properties of fused deposition modelling parts described by classical laminate theory. *Mater Des* 2016;90:453-8. DOI
11. Mohamed OA, Masood SH, Bhowmik JL. Optimization of fused deposition modeling process parameters: a review of current research and future prospects. *Adv Manuf* 2015;3:42-53. DOI
12. Shaqour B, Abuabiah M, Abdel-fattah S, et al. Gaining a better understanding of the extrusion process in fused filament fabrication 3D printing: a review. *Int J Adv Manuf Technol* 2021;114:1279-91. DOI
13. Khudiakova A, Arbeiter F, Spoerk M, Wolfahrt M, Godec D, Pinter G. Inter-layer bonding characterisation between materials with different degrees of stiffness processed by fused filament fabrication. *Addit Manuf* 2019;28:184-93. DOI
14. Li L, Sun Q, Bellehumeur CT, Gu P. Investigation of bond formation in FDM process. *Mater Sci* 2002:400-7. DOI
15. Garzon-hernandez S, Garcia-gonzalez D, Jérusalem A, Arias A. Design of FDM 3D printed polymers: An experimental-modelling methodology for the prediction of mechanical properties. *Mater Des* 2020;188:108414. DOI
16. Ngo TD, Kashani A, Imbalzano G, Nguyen KT, Hui D. Additive manufacturing (3D printing): a review of materials, methods, applications and challenges. *Compos Part B Eng* 2018;143:172-96. DOI
17. Hager I, Golonka A, Putanowicz R. 3D Printing of buildings and building components as the future of sustainable construction? *Procedia Eng* 2016;151:292-9. DOI
18. Colpani A, Fiorentino A, Ceretti E. Design and fabrication of customized tracheal stents by additive manufacturing. *Procedia Manuf* 2020;47:1029-35. DOI
19. Serra T, Capelli C, Toumpaniari R, et al. Design and fabrication of 3D-printed anatomically shaped lumbar cage for intervertebral disc (IVD) degeneration treatment. *Biofabrication* 2016;8:035001. DOI PubMed
20. Cailleaux S, Sanchez-Ballester NM, Gueche YA, Bataille B, Soulairol I. Fused deposition modeling (FDM), the new asset for the production of tailored medicines. *J Control Release* 2021;330:821-41. DOI PubMed
21. Chen G, Xu Y, Chi Lip Kwok P, Kang L. Pharmaceutical applications of 3D printing. *Addit Manuf* 2020;34:101209. DOI PubMed
22. Rajan K, Samykano M, Kadirgama K, Harun WSW, Rahman MM. Fused deposition modeling: process, materials, parameters, properties, and applications. *Int J Adv Manuf Technol* 2022;120:1531-70. DOI
23. Kovan V, Altan G, Topal ES. Effect of layer thickness and print orientation on strength of 3D printed and adhesively bonded single lap joints. *J Mechan Sci Technol* 2017;31:2197-201. DOI
24. Penumakala PK, Santo J, Thomas A. A critical review on the fused deposition modeling of thermoplastic polymer composites. *Compos Part B Eng* 2020;201:108336. DOI
25. Balani S, Chabert F, Nassiet V, Cantarel A. Influence of printing parameters on the stability of deposited beads in fused filament fabrication of poly(lactic) acid. *Addit Manuf* 2019;25:112-21. DOI
26. Sukindar NA, Ariffin MKA, Baharudin BTHT, Jaafar CNA, Ismail MIS. Analyzing the effect of nozzle diameter in fused deposition modeling for extruding polylactic acid using open source 3D printing. *J Teknol* 2016;78:7-15. DOI
27. Triyono J, Sukanto H, Saputra RM, Smaradhana DF. The effect of nozzle hole diameter of 3D printing on porosity and tensile strength parts using polylactic acid material. *Open Eng* 2020;10:762-8. DOI
28. Mwema FM, Akinlabi ET. Basics of fused deposition modelling (FDM), Fused deposition modeling. Cham: Springer International Publishing; 2020. pp. 1-15. DOI
29. Ahn S, Montero M, Odell D, Roundy S, Wright PK. Anisotropic material properties of fused deposition modeling ABS. *Rapid Prototyp J* 2002;8:248-57. DOI
30. Vasudevarao B, Natarajan D, Henderson M. Sensitivity of Rp surface finish to process parameter variation. *Solid Freeform Fabricat Proc* 2000:251-8. DOI
31. Garzon-hernandez S, Arias A, Garcia-gonzalez D. A continuum constitutive model for FDM 3D printed thermoplastics. *Compos Part B Eng* 2020;201:108373. DOI
32. Rajpurohit SR, Dave HK. Analysis of tensile strength of a fused filament fabricated PLA part using an open-source 3D printer. *Int J Adv Manuf Technol* 2019;101:1525-36. DOI
33. Elkholy A, Kempers R. Investigation into the influence of fused deposition modeling (FDM) process parameters on the thermal properties of 3D-printed parts. In Canadian Society for Mechanical Engineering (CSME) International Congress 2018;1-6. DOI
34. Rajpurohit SR, Dave HK. Flexural strength of fused filament fabricated (FFF) PLA parts on an open-source 3D printer. *Adv Manuf* 2018;6:430-41. DOI
35. Çakan BG. Effects of raster angle on tensile and surface roughness properties of various FDM filaments. *J Mech Sci Technol* 2021;35:3347-53. DOI
36. DeCicco A, Faust J. Effect of build parameters on additive materials, graduate theses and dissertations, worcester polytechnic

institute, 2013. Available from: https://web.wpi.edu/Pubs/E-project/Available/E-project-103013-102149 [Last accessed on 29 June 2022].
37. Galantucci L, Lavecchia F, Percoco G. Experimental study aiming to enhance the surface finish of fused deposition modeled parts. *CIRP Annals* 2009;58:189-92. DOI
38. Cabreira V, Santana RMC. Effect of infill pattern in fused filament fabrication (FFF) 3D printing on materials performance. *Matéria* 2020;25:e-12826. DOI
39. Maidin S, Muhamad M, Pei E. Feasibility study of ultrasonic frequency application on fdm to improve parts surface finish. *J Teknol* 2015;77:27-35. DOI
40. Ayrilmis N. Effect of layer thickness on surface properties of 3D printed materials produced from wood flour/PLA filament. *Polym Test* 2018;71:163-6. DOI
41. Reddy V, Flys O, Chaparala A, Berrimi CE, V A, Rosen B. Study on surface texture of Fused Deposition Modeling. *Procedia Manuf* 2018;25:389-96. DOI
42. Pandey PM, Venkata Reddy N, Dhande SG. Improvement of surface finish by staircase machining in fused deposition modeling. *J Mater Process Technol* 2003;132:323-31. DOI
43. Buj-Corral I, Domínguez-Fernández A, Durán-Llucià R. Influence of print orientation on surface roughness in fused deposition modeling (FDM) processes. *Materials* 2019;12:3834. DOI PubMed PMC
44. Wang P, Zou B, Xiao H, Ding S, Huang C. Effects of printing parameters of fused deposition modeling on mechanical properties, surface quality, and microstructure of PEEK. *J Mater Proc Technol* 2019;271:62-74. DOI
45. Anitha R, Arunachalam S, Radhakrishnan P. Critical parameters influencing the quality of prototypes in fused deposition modelling. *J Mater Proc Technol* 2001;118:385-8. DOI
46. Nidagundi V, Keshavamurthy R, Prakash C. Studies on parametric optimization for fused deposition modelling process. *Mater Today Proc* 2015;2:1691-9. DOI
47. Pérez M, Medina-Sánchez G, García-Collado A, Gupta M, Carou D. Surface quality enhancement of fused deposition modeling (fdm) printed samples based on the selection of critical printing parameters. *Materials (Basel)* 2018;11:1382. DOI PubMed PMC
48. Peng T, Yan F. Dual-objective analysis for desktop FDM printers: energy consumption and surface roughness. *Procedia CIRP* 2018;69:106-11. DOI
49. Chohan JS, Kumar R, Yadav A, et al. Optimization of FDM printing process parameters on surface finish, thickness, and outer dimension with ABS polymer specimens using taguchi orthogonal array and genetic algorithms. *Math Prob Eng* 2022;2022:1-13. DOI
50. Kumar SD, Kannan VN, Sankaranarayanan G. Parameter optimization of ABS-M30i parts produced by fused deposition modeling for minimum surface roughness. *Int J Curr Eng Technol* 2014;3:93-7. Available from: https://www.researchgate.net/publication/262529212 [Last accessed on 29 June 2022].
51. Sukindar NA. Optimization of the parameters for surface quality of the open-source 3D printing. *J Mechan Eng* 2017;3:33-3. Available from: https://ir.uitm.edu.my/id/eprint/38508 [Last accessed on 29 June 2022].
52. Lalehpour A, Barari A. Post processing for fused deposition modeling parts with acetone vapour bath. *IFAC-PapersOnLine* 2016;49:42-8. DOI
53. Abbas TF, Othman FM, Ali HB. Influence of layer thickness on impact property of 3D-printed PLA. *Int Res J Eng Technol* 2018;5:1-4. Available from: https://www.irjet.net/archives/V5/i2/IRJET [Last accessed on 29 June 2022].
54. Coogan TJ, Kazmer DO. Bond and part strength in fused deposition modeling. *RPJ* 2017;23:414-22. DOI
55. Rankouhi B, Javadpour S, Delfanian F, Letcher T. Failure analysis and mechanical characterization of 3D printed ABS with respect to layer thickness and orientation. *J Fail Anal Preven* 2016;16:467-81. DOI
56. Leon R, Ling T, Lease J. Optimizing layer thickness and print orientation of 3D objects for enhanced mechanical property using STRUCTO 3D printers. Available from: https://docplayer.net/39789245-Optimizing-layer-thickness-and-print-orientation-of-3d-objects-for-enhanced-mechanical-property-using-structo-3d-printers.html [Last accessed on 29 June 2022].
57. Alafaghani A, Qattawi A, Alrawi B, Guzman A. Experimental optimization of fused deposition modelling processing parameters: a design-for-manufacturing approach. *Procedia Manuf* 2017;10:791-803. DOI
58. Wu W, Geng P, Li G, Zhao D, Zhang H, Zhao J. Influence of layer thickness and raster angle on the mechanical properties of 3D-printed PEEK and a comparative mechanical study between PEEK and ABS. *Materials* 2015;8:5834-46. DOI PubMed PMC
59. Sharma M, Sharma V, Kala P. Optimization of process variables to improve the mechanical properties of FDM structures. *J Phys Conf Ser* 2019;1240:012061. DOI
60. Ramkumar P. Investigation on the effect of process parameters on impact strength of fused deposition modelling specimens. *IOP Conf Ser Mater Sci Eng* 2019;491:012026. DOI
61. Rodríguez-Panes A, Claver J, Camacho AM. The influence of manufacturing parameters on the mechanical behaviour of PLA and ABS pieces manufactured by FDM: a comparative analysis. *Materials* 2018;11:1333. DOI PubMed PMC
62. Hussin R, Abd SZ, Rahim A, et al. Optimization parameter effects on the strength of 3D-printing process using Taguchi method. *AIP Conf Proc Appl Phys Condens Matter* 2019;2129:020154. DOI
63. Vicente CM, Martins TS, Leite M, Ribeiro A, Reis L. Influence of fused deposition modeling parameters on the mechanical properties of ABS parts. *Polym Adv Technol* 2019;31:501-7. DOI
64. Aloyaydi B, Sivasankaran S, Mustafa A. Investigation of infill-patterns on mechanical response of 3D printed poly-lactic-acid. *Polym*

Test 2020;87:106557. DOI
65. Attoye S, Malekipour E, El-mounayri H. Correlation between process parameters and mechanical properties in parts printed by the fused deposition modeling process. In: Kramer S, Jordan JL, Jin H, Carroll J, Beese AM, editors. Mechanics of additive and advanced manufacturing. Cham: Springer International Publishing; 2019. pp. 35-41. DOI
66. Abdelrhman AM, Wei Gan W, Kurniawan D. Effect of part orientation on dimensional accuracy, part strength, and surface quality of three dimensional printed part. *IOP Conf Ser Mater Sci Eng* 2019;694:012048. DOI
67. Eryildiz M. Effect of build orientation on mechanical behaviour and build time of FDM 3D-Printed PLA parts: an experimental investigation. *Eur Mechan Sci* 2021;5:116-20. DOI
68. Vishwas M, Basavaraj C, Vinyas M. Experimental investigation using taguchi method to optimize process parameters of fused deposition modeling for ABS and nylon materials. *Mater Today Proc* 2018;5:7106-14. DOI
69. Raut S, Jatti VS, Khedkar NK, Singh T. Investigation of the effect of built orientation on mechanical properties and total cost of FDM parts. *Procedia Mater Sci* 2014;6:1625-30. DOI
70. Wang P, Zou B, Ding S, Li L, Huang C. Effects of FDM-3D printing parameters on mechanical properties and microstructure of CF/PEEK and GF/PEEK. *Chinese J Aeronaut* 2021;34:236-46. DOI
71. Miazio Ł. Impact of print speed on strength of samples printed in FDM technology. *Agric Eng* 2019;23:33-8. DOI
72. Hwang S, Reyes EI, Moon K, Rumpf RC, Kim NS. Thermo-mechanical characterization of metal/polymer composite filaments and printing parameter study for fused deposition modeling in the 3D printing process. *J Elec Mater* 2015;44:771-7. DOI
73. Pascual A, Toma M, Tsotra P, Grob MC. On the stability of PEEK for short processing cycles at high temperatures and oxygen-containing atmosphere. *Polym Degrad Stab* 2019;165:161-9. DOI
74. Syrlybayev D, Zharylkassyn B, Seisekulova A, Akhmetov M, Perveen A, Talamona D. Optimisation of strength properties of FDM printed parts-a critical review. *Polymers* 2021;13:1587. DOI PubMed PMC
75. Zhou X, Hsieh S, Sun Y. Experimental and numerical investigation of the thermal behaviour of polylactic acid during the fused deposition process. *Virt Phys Prototyp* 2017;12:221-33. DOI
76. Carneiro O, Silva A, Gomes R. Fused deposition modeling with polypropylene. *Mater Des* 2015;83:768-76. DOI
77. Liu X, Zhang M, Li S, Si L, Peng J, Hu Y. Mechanical property parametric appraisal of fused deposition modeling parts based on the gray Taguchi method. *Int J Adv Manuf Technol* 2017;89:2387-97. DOI
78. Abdullah ZZ, Ting HY, Ali MAM, et al. The effect of layer thickness and raster angles on tensile strength and flexural strength for fused deposition modeling (FDM) parts. *J Adv Manuf Technol* 2017;12:147-58. Available from: https://jamt.utem.edu.my/jamt/article/view/4905 [Last accessed on 29 June 2022].
79. Prasada Rao V, Rajiv P, Navya Geethika V. Effect of fused deposition modelling (FDM) process parameters on tensile strength of carbon fibre PLA. *Mater Today Proc* 2019;18:2012-8. DOI
80. Christiyan K, Chandrasekhar U, Rajesh Mathivanan N, Venkateswarlu K. Influence of manufacturing parameters on the strength of PLA parts using layered manufacturing technique: a statistical approach. *IOP Conf Ser Mater Sci Eng* 2018;310:012134. DOI
81. Hasçelik S, Öztürk ÖT, Özerinç S. Mechanical Properties of Nylon Parts Produced by Fused Deposition Modeling. *Int J Mod Manuf Technol* 2021;13:34-8. DOI
82. Palić N, Slavković V, Jovanović Ž, Živić F, Grujović N. Mechanical behaviour of small load bearing structures fabricated by 3D printing. *Appl Eng Lett* 2019;4:88-92. DOI
83. George E, Liacouras P, Rybicki FJ, Mitsouras D. Measuring and establishing the accuracy and reproducibility of 3D printed medical models. *Radiographics* 2017;37:1424-50. DOI PubMed PMC
84. Farias C, Lyman R, Hemingway C, et al. Three-dimensional (3D) printed microneedles for microencapsulated cell extrusion. *Bioengineering (Basel)* 2018;5:59. DOI PubMed PMC
85. Jose PA. 3D Printing of pharmaceuticals-a potential technology in developing personalized medicine. *Asian J Pharm Res Dev* 2018;6:46-54. DOI
86. Galantucci L, Bodi I, Kacani J, Lavecchia F. Analysis of dimensional performance for a 3D open-source printer based on fused deposition modeling technique. *Procedia CIRP* 2015;28:82-7. DOI
87. Sood AK. Study on parametric optimization of fused deposition modelling (FDM) process, graduate theses and dissertations, national institute of technology Rourkela, 2011. Available from: http://ethesis.nitrkl.ac.in/3004/1/Thesis_anoop_kumar_sood_-_507me012.pdf [Last accessed on 29 June 2022].
88. Nancharaiah T, Raju D, Raju V. An experimental investigation on surface quality and dimensional accuracy of FDM components. *Int J Emerg Technol* 2010;1:106-11. Available from: http://citeseerx.ist.psu.edu/viewdoc/summary?doi=10.1.1.670.108 [Last accessed on 29 June 2022].
89. Milde J, Morovič L, Blaha J, Balc N. Influence of the layer thickness in the fused deposition modeling process on the dimensional and shape accuracy of the upper teeth model. *MATEC Web Conf* 2017;137:02006. DOI
90. Xenikakis I, Tzimtzimis M, Tsongas K, et al. Fabrication and finite element analysis of stereolithographic 3D printed microneedles for transdermal delivery of model dyes across human skin in vitro. *Eur J Pharm Sci* 2019;137:104976. DOI PubMed
91. Johnson AR, Procopio AT. Low cost additive manufacturing of microneedle masters. *3D Print Med* 2019;5:2. DOI PubMed PMC
92. Hanon MM, Zsidai L, Ma Q. Accuracy investigation of 3D printed PLA with various process parameters and different colors. *Mater Today Proc* 2021;42:3089-96. DOI
93. Elkaseer A, Schneider S, Scholz SG. Experiment-based process modeling and optimization for high-quality and resource-efficient

FFF 3D printing. *Appl Sci* 2020;10:2899. DOI
94. Valerga AP, Batista M, Fernandez-Vidal SR, Gamez AJ. Impact of chemical post-processing in fused deposition modelling (FDM) on polylactic acid (PLA) surface quality and structure. *Polymers (Basel)* 2019;11:566. DOI PubMed PMC
95. Frunzaverde D, Cojocaru V, Ciubotariu CR, et al. The influence of the printing temperature and the filament color on the dimensional accuracy, tensile strength, and friction performance of FFF-printed PLA specimens. *Polymers (Basel)* 2022;14:1978. DOI PubMed
96. Choi Y, Kim C, Jeong H, Youn J. Influence of bed temperature on heat shrinkage shape error in fdm additive manufacturing of the abs-engineering plastic. *WJET* 2016;4:186-92. DOI
97. Turner N, Strong B, Gold RAS. A review of melt extrusion additive manufacturing processes: i Process design and modeling. *Rapid Prototyp J* 2014;20:192-204. DOI
98. Harris M, Potgieter J, Archer R, Arif KM. In-process thermal treatment of polylactic acid in fused deposition modelling. *Mater Manuf Proc* 2019;34:701-13. DOI
99. Rosli A, Shuib RK, Ishak KMK, Hamid ZAA, Abdullah MK, Rusli A. Influence of bed temperature on warpage, shrinkage and density of various acrylonitrile butadiene styrene (ABS) parts from fused deposition modelling (FDM). *AIP Conf Proce* 2020;2267:020072. DOI
100. Agarwal KM, Shubham P, Bhatia D, Sharma P, Vaid H, Vajpeyi R. Analyzing the impact of print parameters on dimensional variation of ABS specimens printed using fused deposition modelling (FDM). *Sensors Int* 2022;3:100149. DOI
101. Sood AK, Ohdar R, Mahapatra S. Improving dimensional accuracy of fused deposition modelling processed part using grey taguchi method. *Mater Des* 2009;30:4243-52. DOI
102. Padhi SK, Sahu RK, Mahapatra SS, et al. Optimization of fused deposition modeling process parameters using a fuzzy inference system coupled with Taguchi philosophy. *Adv Manuf* 2017;5:231-42. DOI
103. Marwah OMF, Yahaya NF, Darsani A, et al. Investigation for shrinkage deformation in the desktop 3D printer process by using DOE approach of the ABS materials. *J Phys Conf Ser* 2019;1150:012038. DOI
104. Suaidi SNSW, Azizul MAB, Sulaiman SB. The effect of fused deposition modelling process parameters on the quality of abs product. *J Automot Power Transport Technol* 2021;2:45-58. DOI
105. Robles GS, Delda RNM, Del Rosario RLB, Espino MT, Dizon JRC. Dimensional accuracy of 3D - printed acrylonitrile butadiene styrene: effect of size, layer thickness, and infill density. *Key Eng Mater* 2022;913:17-25. DOI
106. Baraheni M, Shabgard MR, Tabatabaee AM, Adhami AH. Practical examining performance of the FDM 3D printed parts. *Res Square* 2022;1:1-25. DOI
107. Chatzidai N, Karalekas D. Experimental and numerical study on the influence of critical 3D printing processing parameters. *Frat Integrità Strutt* 2019;13:407-13. DOI
108. Wickramasinghe S, Do T, Tran P. FDM-based 3D printing of polymer and associated composite: a review on mechanical properties, defects and treatments. *Polymers (Basel)* 2020;12:1529. DOI PubMed PMC
109. Gurrala PK, Regalla SP. Part strength evolution with bonding between filaments in fused deposition modelling: This paper studies how coalescence of filaments contributes to the strength of final FDM part. *Virtual Phys Prototyp* 2014;9:141-9. DOI
110. Seppala JE, Hoon Han S, Hillgartner KE, Davis CS, Migler KB. Weld formation during material extrusion additive manufacturing. *Soft Matter* 2017;13:6761-9. DOI PubMed PMC
111. Huang B, Singamneni S. Raster angle mechanics in fused deposition modelling. *J Compos Mater* 2015;49:363-83. DOI
112. Weeren RV, Agarwala MK, Jamalabad VR, et al. Quality of parts processed by fused deposition. *Mater Sci* 1995. DOI
113. Mali HS, Prajwal B, Gupta D, Kishan J. Abrasive flow finishing of FDM printed parts using a sustainable media. *Rapid Prototyp J* 2018;24:593-606. DOI
114. Lalegani Dezaki M, Mohd Ariffin MKA, Baharuddin BTHT. Experimental study of drilling 3D printed polylactic acid (PLA) in FDM Process. In: Dave HK, Davim JP, editors. Fused Deposition Modeling Based 3D Printing. Cham: Springer International Publishing; 2021. pp. 85-106. DOI
115. Vinitha M, Rao A, Mallik M. Optimization of speed parameters in burnishing of samples fabricated by fused deposition modeling. *Int J Mechan Indust Eng* ;2013:243-5. DOI
116. Žigon J, Karič M, Pavlič M. Surface finishing of 3D-printed polymers with selected coatings. *Polymers (Basel)* 2020;12:2797. DOI PubMed PMC
117. Kumbhar NN, Mulay AV. Post processing methods used to improve surface finish of products which are manufactured by additive manufacturing technologies: a review. *J Inst Eng India Ser C* 2018;99:481-7. DOI
118. Chohan JS, Singh R. Pre and post processing techniques to improve surface characteristics of FDM parts: a state of art review and future applications. *Rapid Prototyp J* 2017;23:495-513. DOI
119. Hashmi AW, Mali HS, Meena A. The surface quality improvement methods for FDM printed parts: a review. In: Dave HK, Davim JP, editors. Fused deposition modeling based 3D printing. Cham: Springer International Publishing; 2021. pp. 167-94. DOI
120. Luzanin O, Movrin D, Plancak M. Experimental Investigation of extrusion speed and temperature effect on arithmetic mean surface roughness in FDM-built specimens. *J Technol Plast* 2013;38:179-90. Available from: https://www.researchgate.net/publication/262255426 [Last accessed on 29 June 2022].
121. Prasad M, Venkatasubbareddy OY, Krishna NJ. Improving the surface roughness of FDM parts by using hybrid methods. *Int J Eng Techni Res* 2019;3:650-4. DOI
122. Akande S. Dimensional accuracy and surface finish optimization of fused deposition modelling parts using desirability function

analysis. *Int J Eng Res Technol* 2015;V4:196-202. DOI

123. Chaidas D, Kitsakis K, Kechagias J, Maropoulos S. The impact of temperature changing on surface roughness of FFF process. *IOP Conf Ser Mater Sci Eng* 2016;161:012033. DOI
124. Kishore KL, Reddy B. Effect of process parameters on the mechanical behavior of FDM processed PLA parts. *Int J Manag Technol Eng* 2018;8:718-23. Available from: http://ijamtes.org/gallery/78 [Last accessed on 29 June 2022].
125. Kovan V, Tezel TÇ, Topal ES, Çamurlu HE. Printing parameters effect on surface characteristics of 3D printed PLA materials. *Int Sci J Mach Technol Mater* 2018;269:266-9. Available from: https://stumejournals.com/journals/mtm/2018/7/266 [Last accessed on 29 June 2022].
126. Velineni A. Investigation on selected factors causing variability in additive manufactured parts, graduate theses and dissertations, Iowa: Iowa State University, 2018. Available from: https://lib.dr.iastate.edu/etd/16891 [Last accessed on 29 June 2022].
127. Jatti VS, Jatti SV, Patel AP, Jatti VS. A study on effect of fused deposition modeling process parameters on mechanical properties. *Int J Sci Technol Res* 2019;8:689-93. Available from: www.ijstr.org [Last accessed on 29 June 2022].
128. Mishra S, Acharya E, Banerjee D, Khan M. An experimental investigation of surface roughness of FDM build parts by chemical misting. *IOP Conf Ser Mater Sci Eng* 2019;653:012043. DOI
129. Jiang J, Xu X, Stringer J. Effect of extrusion temperature on printable threshold overhang in additive manufacturing. *Procedia CIRP* 2019;81:1376-81. DOI
130. Yunus M, Alsoufi MS. Effect of raster inclinations and part positions on mechanical properties, surface roughness and manufacturing price of printed parts produced by fused deposition method. *J Mech Eng Sci* 2020;14:7416-23. DOI
131. Sammaiah P, Rushmamanisha K, Praveenadevi N, Rajasri Reddy I. The influence of process parameters on the surface roughness of the 3D printed part in fdm process. *IOP Conf Ser Mater Sci Eng* 2020;981:042021. DOI
132. Sumalatha M, Malleswara Rao JN, Supraja Reddy B. Optimization of process parameters in 3D printing-fused deposition modeling using taguchi method. *IOP Conf Ser Mater Sci Eng* 2021;1112:012009. DOI
133. Rayegani F, Onwubolu GC. Fused deposition modelling (FDM) process parameter prediction and optimization using group method for data handling (GMDH) and differential evolution (DE). *Int J Adv Manuf Technol* 2014;73:509-19. DOI
134. Shubham P, Sikidar A, Chand T. The influence of layer thickness on mechanical properties of the 3D printed ABS polymer by fused deposition modeling. *Key Eng Mater* 2016;706:63-7. DOI
135. Chacón J, Caminero M, García-plaza E, Núñez P. Additive manufacturing of PLA structures using fused deposition modelling: Effect of process parameters on mechanical properties and their optimal selection. *Mater Des* 2017;124:143-57. DOI
136. Kuznetsov VE, Solonin AN, Urzhumtsev OD, Schilling R, Tavitov AG. Strength of PLA components fabricated with fused deposition technology using a desktop 3D printer as a function of geometrical parameters of the process. *Polymers (Basel)* 2018;10:313. DOI PubMed PMC
137. Benwood C, Anstey A, Andrzejewski J, Misra M, Mohanty AK. Improving the impact strength and heat resistance of 3D printed models: structure, property, and processing correlationships during fused deposition modeling (FDM) of poly(lactic acid). *ACS Omega* 2018;3:4400-11. DOI PubMed PMC
138. Spoerk M, Gonzalez-gutierrez J, Sapkota J, Schuschnigg S, Holzer C. Effect of the printing bed temperature on the adhesion of parts produced by fused filament fabrication. *Plast Rubber Compos* 2017;47:17-24. DOI
139. Ding S, Zou B, Wang P, Ding H. Effects of nozzle temperature and building orientation on mechanical properties and microstructure of PEEK and PEI printed by 3D-FDM. *Polym Test* 2019;78:105948. DOI
140. Khabia S, Jain KK. Influence of change in layer thickness on mechanical properties of components 3D printed on Zortrax M 200 FDM printer with Z-ABS filament material & Accucraft i250+ FDM printer with low cost ABS filament material. *Mater Today Proc* 2020;26:1315-22. DOI
141. Nayak P, Kumar Sahu A, Sankar Mahapatra S. Effect of process parameters on the mechanical behavior of FDM and DMLS build parts. *Mater Today Proce* 2020;22:1443-51. DOI
142. Zhao Y, Zhao K, Li Y, Chen F. Mechanical characterization of biocompatible PEEK by FDM. *J Manuf Proc* 2020;56:28-42. DOI
143. Vălean C, Marşavina L, Mărghitaş M, Linul E, Razavi J, Berto F. Effect of manufacturing parameters on tensile properties of FDM printed specimens. *Procedia Struct Integr* 2020;26:313-20. DOI
144. Yadav DK, Srivastava R, Dev S. Design & fabrication of ABS part by FDM for automobile application. *Mater Today Proc* 2020;26:2089-93. DOI
145. Ouballouch A, alaiji RE, Ettaqi S, Bouayad A, Sallaou M, Lasri L. Evaluation of dimensional accuracy and mechanical behavior of 3D printed reinforced polyamide parts. *Procedia Struct Integr* 2019;19:433-41. DOI
146. Azhikannickal E, Uhrin A. Dimensional stability of 3D printed parts: effects of process parameters. *Ohio J Sci* 2019;119:9. DOI